1979

Synthesis and structure of two octahedral molybdenum chloride sulfide clusters

John Byrne Michel
Iowa State University

INFORMATION TO USERS

This was produced from a copy of a document sent to us for microfilming. While the most advanced technological means to photograph and reproduce this document have been used, the quality is heaviiy dependent upon the quality of the material submitted.

The following explanation of techniques is provided to help you understand markings or notations which may appear on this reproduction.

1. The sign or "target" for pages apparently lacking from the document photographed is "Missing Page(s)". If it was possible to obtain the missing page(s) or section, they are spliced into the film along with adjacent pages. This may have necessitated cutting through an image and duplicating adjacent pages to assure you of complete continuity.

2. When an image on the film is obliterated with a round black mark it is an indication that the film inspector noticed either blurred copy because of movement during exposure, or duplicate copy. Unless we meant to delete copyrighted materials that should not have been filmed, you will find a good image of the page in the adjacent frame.

3. When a map, drawing or chart, etc., is part of the material being photographed the photographer has followed a definite method in "sectioning" the material. It is customary to begin filming at the upper left hand corner of a large sheet and to continue from left to right in equal sections with small overlaps. If necessary, sectioning is continued again—beginning below the first row and continuing on until complete.

4. For any illustrations that cannot be reproduced satisfactorily by xerography, photographic prints can be purchased at additional cost and tipped into your xerographic copy. Requests can be made to our Dissertations Customer Services Department.

5. Some pages in any document may have indistinct print. In all cases we have filmed the best available copy.

University
Microfilms
International

300 N. ZEEB ROAD, ANN ARBOR, MI 48106
18 BEDFORD ROW, LONDON WC1R 4EJ, ENGLAND

MICHEL, JOHN BYRNE

SYNTHESIS AND STRUCTURE OF TWO OCTAHEDRAL MOLYBDENUM CHLORIDE SULFIDE CLUSTERS

Iowa State University PH.D. 1979

Synthesis and structure of two octahedral molybdenum chloride sulfide clusters

by

John Byrne Michel

A Dissertation Submitted to the
Graduate Faculty in Partial Fulfillment of
The Requirements for the Degree of
DOCTOR OF PHILOSOPHY

Department: Chemistry
Major: Inorganic Chemistry

Approved:

Signature was redacted for privacy.

In Charge of Major Work

Signature was redacted for privacy.

For the Major Department

Signature was redacted for privacy.

For the Graduate College

Iowa State University
Ames, Iowa

1979

TABLE OF CONTENTS

LIST OF FIGURES

LIST OF TABLES

INTRODUCTION

Statement of the Problem

Since the initial report by Chevrel and co-workers[1] of a new class of binary and ternary molybdenum chalcides Mo_6Y_8 and $M_nMo_6Y_8$ (Y=chalcide; M=metal cation), the preparations,[2-6] structures,[7-12] and physical properties[13-17] of a large number of derivatives have been reported. This extensive activity was spurred on by the discovery that many of these "Chevrel phases" are superconductors.[18]

The structures of all the Chevrel phases consist of interconnected Mo_6Y_8 clusters. The Mo_6Y_8 cluster is closely related to the $Mo_6X_8^{4+}$ (X=halide) cluster of the α-molybdenum(II) halides.[19] Since the Mo_6X_8 cluster exists in both a chalcide (Mo_6Y_8) and a halide ($Mo_6X_8^{4+}$) form, halide-chalcide clusters $Mo_6X_{8-n}Y_n$ might also form stable compounds. The goal of this research project was the preparation and characterization of these halide-chalcide clusters.

Structure of the Mo_6X_8 Cluster

An isolated Mo_6X_8 cluster unit, illustrated in Figure 1, consists of six molybdenum atoms bonded together forming an octahedral cluster, along with eight ligand atoms (halide or chalcide), each centered above one of the eight octahedral faces. These eight atoms are termed "bridging ligands" because each bridges the three molybdenum atoms which comprise each octahedral face. From a different point of view, the eight bridging ligands define the vertices of a cube, with a molybdenum atom near the center of each face. The entire unit has idealized O_h point group symmetry. The cluster has six coordination sites, each within bonding distance of a molybdenum atom. The sites are located outside the cube on the normals to the six faces of the cube. If these coordination sites are occupied by bridging ligands of neighboring clusters, the result is extensive bonding between clusters. This arrangement occurs in the structures of the Chevrel phases. In the structures of the α-molybdenum(II) halides and their derivatives, the cluster's coordination sites are occupied by "terminal ligands". Although each of these terminal ligands may be shared between a pair of clusters, they still block the close approach among neighboring clusters found in the Chevrel phase structure. In order to

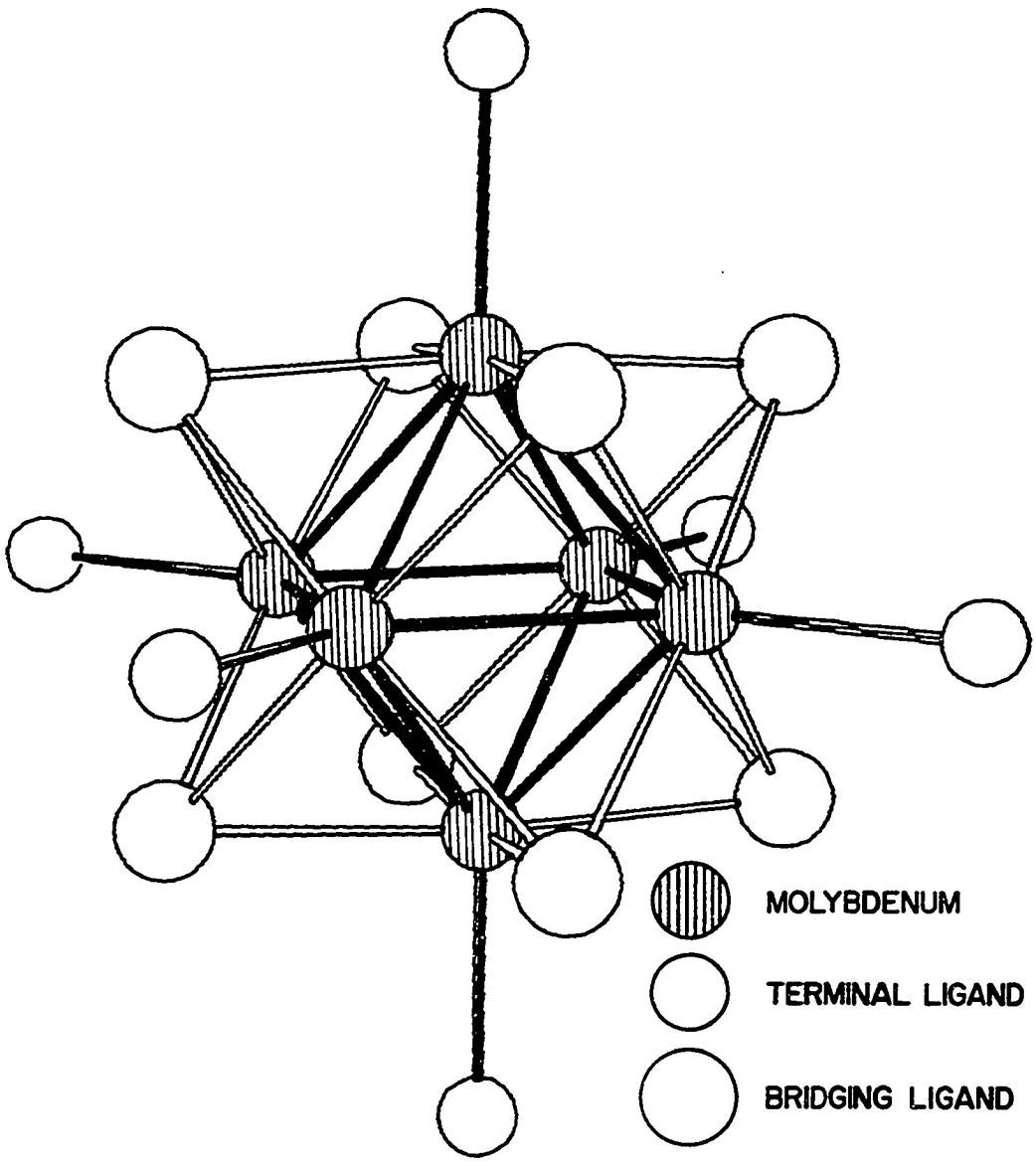

Figure 1. A perspective view of the Mo_6X_8 cluster

clarify the reader's view of the structures of these two classes of compounds, the structures of two α-molybdenum(II) halide compounds and two Chevrel phases will be described in detail in the following two parts of the introduction.

Structure of the α-molybdenum(II) halides and derivatives

The structures of Mo_6Cl_{12} and $Mo_6Br_{12}(H_2O)_2$ are excellent archetypes of the structures adopted by the α-molybdenum(II) halides and their derivatives. Extensive sharing of terminal ligands occurs in the structure of Mo_6Cl_{12}; on the other hand, the structure of $Mo_6Br_{12}(H_2O)_2$ consists of discrete, isolated clusters.

Although Mo_6Cl_{12} crystallizes in the orthorhombic space group Bbam,[19] the $Mo_6Cl_8^{4+}$ cluster has idealized O_h symmetry. The two Mo-Mo bond lengths are 2.604 and 2.608Å,[20] reflecting a slight tetragonal elongation. The average Mo-Mo bond (2.607Å) is slightly longer than the sum of the metallic radii (2.59Å).[21] The nonbonded Cl_b-Cl_b distances between bridging chlorides are between 3.481 and 3.496Å, average value of 3.491Å. This distance is only 0.11Å shorter than the sum of the van der Waals radii.[22] The molybdenum atoms are displaced 0.11Å out from the faces of the cube. The Mo-Cl_b distances in the $Mo_6Cl_8^{4+}$ unit fall between 2.469Å and 2.474Å, and the average Mo-Cl_b-Mo angle is 63.69Å.

The arrangement of terminal ligands in the cluster's coordination sites reduces the "molecular" symmetry to pseudo tetragonal. The four coordination sites in the plane perpendicular to the pseudo 4-fold axis are occupied by terminal ligands which are each shared equally with a neighboring cluster. Thus, each cluster is linked through these four shared terminal ligands to four neighboring clusters by long $Mo\text{-}Cl_{tt}$ bonds (2.494Å). The cluster's two remaining coordination sites, located on the pseudo 4-fold axis, are occupied by terminal ligands (unshared), with a $Mo\text{-}Cl_t$ bond length of 2.379Å. This bond is significantly shorter and stronger than the $Mo\text{-}Cl_{tt}$ bond. The greater strength of the $Mo\text{-}Cl_t$ bond is reflected by the slight tetragonal elongation of the Mo_6 octahedron. The explanation of this assertion follows. Since the p_z atomic orbitals on molybdenum used for bonding to the terminal ligands are pointed toward the center of the cluster, they are also of proper symmetry for Mo-Mo bonding. Assuming that the four $Mo\text{-}Cl_{tt}$ bonds are weak relative to the two $Mo\text{-}Cl_t$ bonds, the p_z orbitals on each of the four molybdenum atoms are more available to supplement the Mo-Mo bonding than their counterparts on the other two molybdenum atoms. Because of the orientation of these four orbitals, only the four Mo-Mo bonds in the plane perpendicular to the pseudo 4-fold rotation axis

would be strengthened. Thus, these four bonds would be shorter than the other eight, corresponding to a tetragonal elongation.

Despite the sharing of terminal chloride ligands, the closest approach between molybdenum atoms of neighboring clusters is 4.54Å, far outside the range of any direct interaction. These bridges between clusters are easily ruptured. Reaction of molybdenum dichloride with a donor ligand L yields discrete $(Mo_6Cl_8)Cl_4L_2$ clusters.

$(Mo_6Br_8)Br_4(H_2O)_2$ is a structurally characterized bromide analog of this type of derivative.[23] Although this compound crystallizes in the tetragonal space group I4/m, the $Mo_6Br_8^{4+}$ cluster has idealized octahedral point group symmetry. The Mo-Mo bond lengths are 2.640 and 2.630Å. These bonds are slightly longer than the Mo-Mo bonds in Mo_6Cl_{12}. The $Mo-Br_b$ bond lengths of $Mo_6Br_8^{4+}$ are 2.601Å, on the average. This bond is 0.13Å longer than the $Mo-Cl_b$ bond of Mo_6Cl_{12}, in good agreement with the increased tetrahedral covalent radius of bromine[24] (0.12Å larger than chlorine). The average Br_b-Br_b nonbonded distance of the $Mo_6Br_8^{4+}$ unit is 3.679Å, 0.23Å shorter than the sum of the van der Waals radii.[22] With this larger cube, the Mo atoms lie only 0.03-0.04Å above the cube faces.

The entire molecule, including the terminal ligands, has crystallographically imposed C_{4h} symmetry. The two water

molecules coordinated to the cluster occupy the terminal ligand sites on the cluster's 4-fold rotation axis. The Mo-O bond length is 2.191Å, 0.13Å larger than the value estimated by addition of covalent radii.[25,26] The Mo-Br_t bond length is 2.587Å, slightly longer than the 2.54Å estimated value.[25,26]

Despite the very different extents of intercluster linkage in these two compounds, the strength of corresponding bonds in the $Mo_6X_8^{4+}$ units is very similar.

Structure of the Chevrel phases

The Chevrel phases are a series of binary and ternary molybdenum chalcides Mo_6Y_8 and $M_nMo_6Y_8$ (Y=S, Se, Te; M=metal cation; n=0 to 4). The ternary compounds are formally derived from the binary phases by insertion of metal cations into holes in the binary lattice. The structures of Mo_6S_8 and of $PbMo_6S_8$[27] will be described in order to illustrate changes in the structure of the Mo_6S_8 lattice upon insertion of a metal cation.

Mo_6S_8 crystallizes in the rhombohedral space group $R\bar{3}$, with Z=1.[10] Each Mo_6S_8 cluster has been elongated along its 3-fold rotation axis, and has crystallographically imposed S_6 symmetry. The two Mo-Mo bond lengths are 2.698Å and 2.862Å, 2.780Å average. This average Mo-Mo bond is 0.17Å

longer than the bond in Mo_6Cl_{12}. The Mo-Mo bonding in Mo_6S_8 is expected to be weaker than in Mo_6Cl_{12}, because Mo_6S_8 has only 20 electrons in its Mo-Mo bonding orbitals, while Mo_6Cl_{12} has 24. The S-S distances along edges of the distorted S_8 cube are 3.310Å and 3.550Å, 3.430Å average. The average S-S distance is 0.06Å shorter than the Cl-Cl distance of Mo_6Cl_{12}. The Mo atoms are located 0.25Å above the faces of the S_8 cube. The Mo-S_b distances are between 2.426 and 2.460Å. The average Mo-S_b bond length of Mo_6S_8 (2.439Å) is 0.032Å shorter than the Mo-Cl_b bond length of Mo_6Cl_{12}. Since the covalent radius of sulfur is 0.05Å larger than that of chlorine,[24] the Mo-S_b bond of Mo_6S_8 is significantly stronger than the Mo-Cl_b bond of Mo_6Cl_{12}.

Two of the eight bridging sulfides of Mo_6S_8 occupy special positions (site symmetry 3) in the unit cell. The Mo-S_b-Mo angles are 67.2° for these two sulfides. The intracluster Mo-S_b-Mo angles of the other six bridging sulfides (in general unit cell positions) are 70.3°, on the average. These angles are 3.5° to 6.6° larger than the corresponding angles of Mo_6Cl_{12}, reflecting the stronger bond between molybdenum and the bridging ligand in Mo_6S_8. Each of the six sulfides in general cell positions, in addition to its role as an intracluster bridging ligand, serves as a "terminal ligand" for a molybdenum atom of one of the six neighboring clusters. The Mo-S_{tb} bond length is 2.425Å. Again taking

the larger covalent radius of sulfur into account, this bond is as strong as the two strong Mo-Cl_t bonds of Mo_6Cl_{12} (2.379Å). This mode of filling the cluster's coordination sites is responsible for the strong intercluster bonding in the structure of Mo_6S_8. As illustrated in Figure 2, each cluster is linked to each of its six neighboring clusters by two strong Mo-S_{tb} bonds. The intercluster Mo-Mo distance of 3.08Å is much shorter than the corresponding 4.54Å distance of Mo_6Cl_{12}, and indicates significant interaction.

Like most of the ternary Chevrel phases, $PbMo_6S_8$ is isomorphous with Mo_6S_8.[9] Its structure consists of a distorted Mo_6S_8 lattice with Pb atoms inserted into some of the holes. The flexibility of the Mo_6S_8 lattice is demonstrated by comparing the structures of Mo_6S_8 and $PbMo_6S_8$.

The trigonal elongation of the Mo_6S_8 clusters is less severe in the structure of $PbMo_6S_8$ than in the Mo_6S_8 structure. Thus, the two Mo-Mo bond lengths (2.737 and 2.672Å) are more nearly equal in $PbMo_6S_8$, as are the edges of the S_8 "cube" (3.428, 3.488Å). By comparison of structural data from a variety of Chevrel phases, Yvon has shown that the trigonal distortion of the Mo_6S_8 clusters decreases as the number of electrons available for Mo-Mo bonding increases.[28] $PbMo_6S_8$ formally has 22 Mo-Mo bonding electrons, while Mo_6S_8 has 20. The averaged Mo-Mo bond in $PbMo_6S_8$ is shorter than in Mo_6S_8

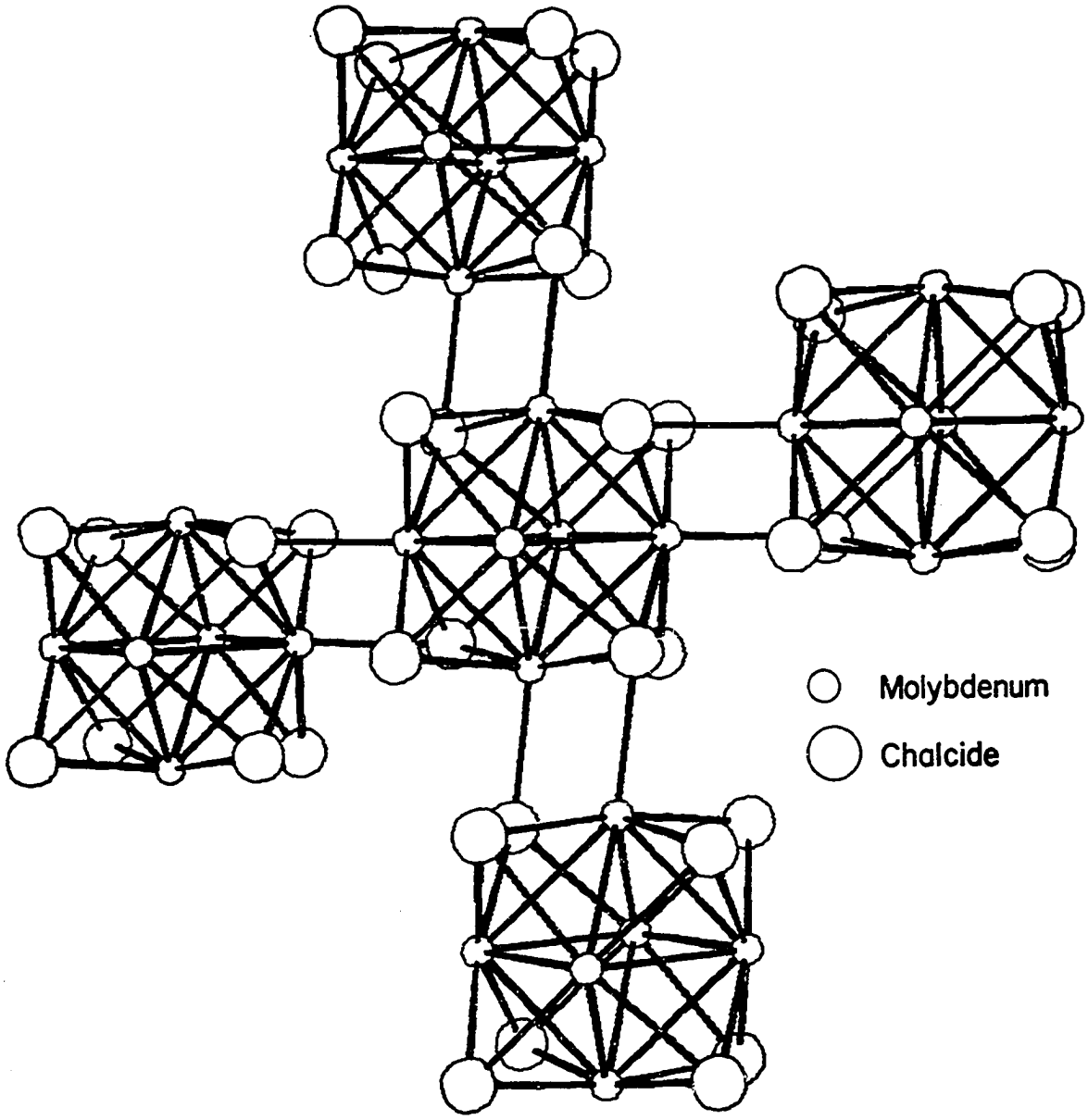

Figure 2. A perspective view of the arrangement of Mo_6X_8 clusters in the Chevrel phases, with two of the six neighboring clusters deleted

(2.705 and 2.780Å, respectively), due also to the increased number of Mo-Mo bonding electrons in $PbMo_6S_8$.

The Mo-S_b bond lengths are 2.455Å (average), only 0.016Å longer than in Mo_6S_8. The intracluster Mo-S_b-Mo angles are 67.96° for the two bridging sulfides in special positions, 66.55° (average) for the other six sulfides. The Mo-S_{tb} bond is much longer than in Mo_6S_8 (2.566 vs. 2.426Å), demonstrating that insertion of the large Pb^{2+} ions into the lattice pushes neighboring Mo_6S_8 clusters apart. The weakened intercluster bonding is further underscored by the increase in the intercluster Mo-Mo distance from 3.08Å in Mo_6S_8 to 3.26Å in $PbMo_6S_8$. The superconducting properties of the Chevrel phases are a sensitive function of the bonding between clusters.[28] Significantly, although Mo_6S_8 is not a superconductor, $PbMo_6S_8$ has the highest superconducting transition temperature measured for the Chevrel phases (T_c=15.2°K).[9]

The Pb^{2+} ions in the structure are located at the origin of the rhombohedral unit cell. The overall structure can be viewed as a distorted body-centered cubic lattice, with Mo_6S_8 clusters at the corners of the cell and Pb^{2+} ions at the body center. The Pb^{2+} ions are surrounded by a distorted cube of sulfides, each a bridging ligand of one of the eight surrounding Mo_6S_8 clusters. The Pb-S distance for the six sulfides in general positions is 3.117Å, for the two sulfides

in special positions 2.786Å. The shortest Mo-Pb distance is 4.23Å.

As in $PbMo_6S_8$, the metal cation in the ternary Chevrel phases generally exerts only an indirect influence on the Mo_6S_8 intracluster bonding, i.e., strengthening of the Mo-Mo bonding by donation of its valence electrons to the Mo-Mo bonding orbitals. However, it directly affects the intercluster bonding and the number of electrons in the conduction band (which consists of Mo-Mo bonding orbitals), both of which are critical determinants of the compound's electronic conduction properties.

Bonding

The purpose of this discussion is to compare the qualitative results of descriptions of the bonding in the α-molybdenum(II) halides and the Chevrel phases. Cotton and Haas were the first to use molecular orbitals formed from linear combinations of atomic orbitals to describe the Mo-Mo bonding in M_6X_8 clusters.[29] Their model was an octahedral $Mo_6Cl_8^{4+}$ cluster, with the coordinate system on each molybdenum atom oriented so that its z axis pointed toward the center of the octahedron, and its x and y axes pointed over octahedral edges. This orientation has also been used in the other bonding schemes described below. The orbitals on each molybdenum atom were assigned the following roles:

a) $5s$, $4p_x$, $4p_y$, $4d_{xy}$ for Mo-Cl_b bonding;

b) $5p_z$ for Mo-Cl_t or Mo-Cl_{tt} bonding. These five orbitals on each molybdenum were excluded from the calculation;

c) $4d_{x^2-y^2}$, $4d_{xz}$, $4d_{yz}$, $4d_{z^2}$ for Mo-Mo bonding.

Mixing of ligand orbitals with the Mo-Mo orbitals was neglected, because of the presumed large energy gap between these two sets of orbitals. Linear combinations of the twenty-four atomic orbitals were formed; twelve Mo-Mo bonding and twelve Mo-Mo antibonding orbitals resulted. The 24 electrons available for Mo-Mo bonding in Mo_6Cl_{12} and its derivatives exactly fill the 12 bonding orbitals. Since a Mo_6 octahedron has 12 Mo-Mo bonds (12 octahedral edges), each bond has an order of one. Confirming this, the Mo-Mo bond length of Mo_6Cl_{12} (2.607Å) is only 0.02Å longer than the value calculated by doubling the metallic radius of molybdenum.[21]

A critical approximation made by Cotton and Haas was to neglect the mixing of ligand orbitals with the Mo-Mo bonding orbitals. The validity of this approximation, dependent upon the large difference in energy between the atomic orbitals of chlorine and the molybdenum 4d orbitals, becomes increasingly suspect in the cases of the $Mo_6Br_8^{4+}$ and $Mo_6I_8^{4+}$ clusters. Guggenberger and Sleight demonstrated the importance of this mixing in their description of the Mo-Mo bonding in $(Mo_6Br_8)Br_4(H_2O)_2$.[23] Applying an extended Hückel approach to the

$Mo_6Br_8^{4+}$ cluster, they also derived a set of twelve bonding and twelve antibonding Mo-Mo orbitals. As with the Cotton and Haas scheme, the two highest-lying bonding orbitals (T_{2u} and E_g) were both composed of $4d_{x^2-y^2}$ orbitals. However, in the Cotton and Haas scheme, the E_g was lower in energy than the T_{2u} orbital; Guggenberger and Sleight found that the E_g orbital was the highest-energy bonding orbital. The destabilization of the E_g orbital (with respect to the Cotton and Haas scheme) can be attributed to mixing with the ligand orbitals, because this orbital had the largest Br contribution of the Mo-Mo bonding orbitals. Inclusion of terminal ligand orbitals in the calculation destabilized all the Mo-Mo bonding orbitals, but the order (according to energy) of the orbitals remained the same.

The schemes of Cotton and Haas and of Guggenberger and Sleight both predict that the most stable electron configuration for the α-molybdenum(II) halides and their derivatives has 24 electrons filling the 12 Mo-Mo bonding orbitals. Experimentally, there is only one possible exception. Hamer, Smith and Walton have indirect evidence for the 26 electron $(Mo_6Cl_8)^{2+}$ cluster in a compound formulated as $[(Mo_6Cl_8)(P(CH_2CH_3)_3)_6][(Mo_6Cl_8)Cl_6]$.[30]

Assessing the bonding in the Chevrel phases is a more difficult problem, because of the extensive bonding between clusters. Nevertheless, on a qualitative level, the bonding

scheme developed by Andersen et al.[31] is quite analogous to the previously described schemes for the α-Mo(II) halides. Andersen et al. used a linear-combination-of-muffin-tin-orbitals method, with the atomic sphere approximation to describe the bonding in Mo_6S_8, Mo_6Se_8, and $PbMo_6S_{7.5}$. The energies of the molecular orbitals formed by overlap of the thirty molybdenum d orbitals of an isolated Mo_6 cluster were first computed. Thirteen bonding molecular orbitals resulted, with relative energies similar to the ordering derived by Cotton and Haas. When the weak bonding between molybdenum atoms of neighboring clusters was included in the calculation, the molecular orbitals of the isolated octahedron merged into a number of narrow "sub-bands". The final refinement applied to the calculation was mixing of the molybdenum orbitals with the 3p orbitals of the bridging and "terminal" sulfides. The energies and widths of some of the bands were drastically affected. Most importantly, the energy of an A_u Mo-Mo bonding orbital of d_{xy} character was greatly increased, so that the orbital became antibonding. At the top of the envelope of 12 Mo-Mo bonding orbitals, the E_g orbital ($d_{x^2-y^2}$) mixed strongly with the intracluster sulfur 3p orbitals, was shifted above the T_{2u} ($d_{x^2-y^2}$) orbital, and so became the highest-energy Mo-Mo bonding orbital. Thus, Andersen's scheme is qualitatively very similar to the scheme developed by Guggenberger and Sleight:

1) Up to 24 electrons can be accommodated by 12 Mo-Mo bonding orbitals;

2) The two Mo-Mo bonding orbitals of highest energy are both derived from Mo $4d_{x^2-y^2}$ atomic orbitals;

3) The E_g orbital is the highest energy bonding orbital.

The E_g sub-band is the major component of the conduction band in all three of the Chevrel phases studied. Varying degrees of overlap of the E_g band with lower-lying sub-bands occur in all three compounds. Thus, although the E_g sub-band is formally empty in the binary Chevrel phases (20 electrons available for Mo-Mo bonding), because of the overlap, these compounds are electrical conductors. There are 22-24 Mo-Mo bonding electrons per cluster in the ternary Chevrel phases, with the additional 2-4 electrons going into the conduction band.[28] As expected from the calculation, Chevrel phases with full conduction bands (24 electrons per cluster) are semiconductors.[32] The rest of the ternary Chevrel phases are metallic, and most are superconductors.[28] The Mo-Mo bonding character of the orbitals which make up the conduction band is reflected by a contraction of the intracluster Mo-Mo bonds as the conduction band is filled.

Preparations and Chemistry of the Chevrel Phases

With few exceptions, all of the Chevrel phases are prepared by heating a pelletized stoichiometric mixture of molybdenum metal and elemental chalcogen (plus an additional

component for the ternary Chevrel phases, as described below) at temperatures between 900-1200°C for ca. 24 hours in a sealed evacuated quartz ampoule.[1-6]

The ternary Chevrel phases can be conveniently divided into three categories. Those in the first can be formally derived (in some cases experimentally derived) from the binary Chevrel phases by insertion of metal cations into holes in the binary structure. A large number of ternary sulfides and selenides $M_nMo_6Y_8$ has been prepared by adding elemental M, or MY in some cases, to the reaction mixture. Some examples to indicate the variety of cations and stoichiometries are:[28]

Y=S; M(n)=Fe(1.32), Co(1.6), Ni(0.4, 2.0), Cu(1.8, 2.76, 2.94, 3.66), Ag(1.0), In(1.0), Sn(1.0), Pb(0.92, 1.0), La(1.0), Gd(1.0), Ho(1.0), Er(1.0);

Y=Se; M(n)=Cu(1.0, 1.5, 2.0), Ag(1.0), Sn(0.8), Pb(1.0), La(0.85).

As mentioned, some of these compounds can be prepared by thermal[33] or electrochemical[5] insertion of ternary metal cations into a binary Chevrel phase.

The second category consists of the two compounds $Mo_6S_6Br_2$ and $Mo_6S_6I_2$, prepared by adding MoX_2(X=Br, I) to the reaction mixture.[34] Both compounds are formally derived from Mo_6S_8 by replacing 2 of the bridging sulfides with halides. The authors speculated that the halides occupy the 2 special bridging ligand sites on the 3-fold axis of the

unit cell. In this case, the two halides would be coordinated to three molybdenum atoms; if they occupied one of the other bridging ligand sites, their coordination number would be four, unfavorably high.

The third category consists of the three compounds $Re_4Mo_2S_8$, $Re_4Mo_2Se_8$, and $Re_2Mo_4Te_8$, all formally derived from the binary Chevrel phases by replacing some of the Mo atoms with Re. They are prepared by adding Re metal to the reaction mixture.[32] $Re_4Mo_2Y_8$ (Y=S, Se) are the only Chevrel phases with exactly 24 Mo-Mo bonding electrons per cluster, and both compounds are semiconductors.

Many of the ternary Chevrel phases are nonstoichiometric. $Mo_6S_6I_2$ and $Mo_6S_6Br_2$ are both ca. 13% deficient in halogen. Among the ternary Chevrel phases of the first category ($M_nMo_6S_8$), nonstoichiometry is not limited to the ternary metal atoms. For example, in an investigation of the phase diagram of $Pb_xMo_6S_y$, Hauck observed that both x and y have finite ranges ($0.85 \leq x \leq 1.05$; $6.8 \leq y \leq 7.4$).[35] There is some controversy over the causes of the nonstoichiometry in this compound. In their refinement of the crystal structure of $Pb_{0.92}Mo_6S_{7.5}$, Marezio et al. observed a deficiency at the Pb^{2+} site and at the sulfide (special position) site.[9] In a more recent examination of this compound, chemical analysis and density measurements indicated an excess of molybdenum, with normal sulfur and lead contents.[6] Since the superconducting properties of many of the Chevrel phases are

noticeably variant among different samples of the same compound, further research relating the details of the preparative procedure to the stoichiometry is needed.

Thus, a wide variety of Chevrel phases has been prepared using this simple preparative procedure. However, Mo_6S_8 could not be prepared in this way because it is not thermodynamically stable above 468°C.[10] Mo_6S_8 was synthesized by leaching the Ni^{2+} cations out of the $Ni_2Mo_6S_8$ lattice in hydrochloric acid solution. The development of alternative, lower temperature syntheses might lead to new compounds (e.g., W_6S_8) which might not be accessible via the general procedure. Some recent work by Schöllhorn et al. supports this contention.[5] They prepared previously unreported alkali metal derivatives of Mo_6S_8 ($M_xMo_6S_8$; M=Li, Na; $0 < x < 3.6$) by electrochemical reduction of Mo_6S_8 electrodes in 1,2-dimethoxyethane solutions of the alkali metal cations.

Chemistry of α-Molybdenum(II) Chloride

Because the syntheses of α-molybdenum(II) chloride have been described elsewhere,[36] they will not be considered here. Instead, this discussion will be focussed on the chemistry of Mo_6Cl_{12} and its derivatives.

The cluster unit of α-molybdenum(II) chloride is remarkably stable. One indication of this stability is that Mo_6Cl_{12} is not oxidized when treated with hot concentrated nitric acid.[19] The cluster can be decomposed by aqueous

solutions of vigorous nucleophiles like fluoride or hydroxide.[37] The key to this decomposition is preliminary substitution of these nucleophiles into the cluster's bridging ligand sites. Less reactive nucleophiles can be substituted into the cluster's ligand sites (bridging or terminal), but without subsequent cluster decomposition. Since these ligand substitution reactions comprise the bulk of the non-degradative chemistry of Mo_6Cl_{12}, these reactions will be considered in detail.

The most reactive components of Mo_6Cl_{12} are the four shared terminal chlorides on each cluster which bridge to neighboring clusters. These bridges are easily ruptured by a variety of donor ligands:[38,39,40]

$$(Mo_6Cl_8)Cl_{4/2}Cl_2 + 2L \longrightarrow (Mo_6Cl_8)Cl_4L_2$$

$$L=H_2O,\ C_5H_5N,\ (H_3C)_2SO,\ (H_3C)_2NCOH,\ \text{etc.}$$

The terminal ligands are quite labile. Lessmeister and Schäfer have investigated the kinetics of bromide substitution into the terminal ligand sites in aqueous hydrohalic acid solution.[41] The substitution proceeds in two steps:

$$(Mo_6Cl_8)Cl_6^{2-} + H_2O \longrightarrow (Mo_6Cl_8)Cl_5(H_2O)^- + Cl^-$$

$$(Mo_6Cl_8)Cl_5(H_2O)^- + Br^- \longrightarrow (Mo_6Cl_8)Cl_5Br^{2-} + H_2O\,.$$

The aquation step is rate determining, with a rate constant $k = 7 \times 10^{-4}$ sec^{-1}. In this case, with two very similar ligands competing for the terminal ligand sites, the substitution is statistically controlled (i.e., substitution at a site is not influenced by neighboring sites). Three types of derivatives of Mo_6Cl_{12} have been prepared via terminal ligand substitution reactions:

1) $(Mo_6Cl_8)Cl_4 + 4\ AgClO_4 \xrightarrow{CH_3OH} 4\ AgCl +$

$"[(Mo_6Cl_8)(CH_3OH)_6](ClO_4)_4"$

$"[(Mo_6Cl_8)(CH_3OH)_6](ClO_4)_4" + 6L \xrightarrow{CH_3OH}$

$[(Mo_6Cl_8)L_6](ClO_4)_4$ L=DMF, DMSO[38];

2) $(Mo_6Cl_8)Cl_4 + 6HX \xrightarrow[H_2O]{C_2H_5OH} (H_3O)_2[(Mo_6Cl_8)X_6] + 4HCl$

X=Br, I, N_3, NCS, etc.[42,43];

3) $(H_3O)_2[(Mo_6Cl_8)X_6] \xrightarrow{350°C} (Mo_6Cl_8)X_4 + 2H_2O + 2HX$

X=Cl, Br, I[43].

Substitution at the cluster's bridging ligand sites has also been investigated. Since each bridging chloride forms three strong Mo-Cl_b bonds, these ligands are much less labile than the terminal ligands. Thus, although it has been shown that substitution at the bridging ligand sites occurs at room

temperature in dilute hydrohalic acid solutions (ca. 1.5M), it is much too slow to be a useful preparative reaction.[41]

More forcing reaction conditions are required to improve the synthetic utility of halide substitution into the bridging ligand sites of $Mo_6Cl_8^{4+}$. Sheldon found that complete halogen exchange occurred when Mo_6Cl_{12} was dissolved in anhydrous LiX (X=Br, I) melts:

$$Mo_6Cl_{12} + 12LiX \longrightarrow Mo_6X_{12} + 12LiCl^{44}.$$

Baumann, Plautz and Schäfer observed intramolecular bridging-terminal ligand exchange when the mixed halides $(Mo_6Cl_8)X_4$ (X=Br, I) were tempered at 400°C for 2 weeks:

$$(Mo_6Cl_8)X_4 \longrightarrow (Mo_6X_4Cl_4)Cl_4^{43}.$$

In these experiments of Sheldon and Baumann et al., a heavier halide preferentially displaced a lighter halide from a bridging ligand site. Lesaar and Schäfer later demonstrated that a lighter halide displaced a heavier halide from a bridging ligand site when α-molybdenum(II) halides were dissolved in Hg(II) halide melts:[45]

$$(Mo_6X_8)X_4 + 7HgY_2 \longrightarrow Hg[(Mo_6Y_8)Y_6] + 6HgX_2$$

X=I; Y=Br, Cl

X=Br; Y=Cl.

The change in direction of the bridging ligand substitution was explained on simple thermodynamic grounds.

Attempts to substitute nonhalides into the bridging ligand sites of α-molybdenum(II) chloride have been generally less successful. Both Sheldon and Baumann et al. showed that one or two hydroxide ions can be substituted into bridging ligand sites;[43,46] attempts to increase the extent of the substitution were thwarted by cluster decomposition. The only example of extensive bridging ligand substitution by a nonhalide was provided by Nannelli and Block. They prepared $Na_2[(Mo_6(OCH_3)_8)(OCH_3)_6]$ by heating a methanol solution of Mo_6Cl_{12} and $NaOCH_3$ to dryness.[47] The product was well-characterized, but quite unstable.

Topotactic oxidation-reduction chemistry of α-molybdenum(II) chloride is nonexistent, with one possible exception. Hamer, Smith and Walton have reported the reduced, 26 electron cluster $(Mo_6Cl_8)^{2+}$, isolated in a compound formulated as $[(Mo_6Cl_8)(P(CH_2CH_3)_3)_6][(Mo_6Cl_8)Cl_6]$.[30] The compound resulted from an extended reaction between α-molybdenum(II) chloride and triethylphosphine in ethanol, and was characterized by means of infrared, Raman, and photoelectron spectra.

The goal of this research is the preparation and characterization of sulfide-chloride clusters $Mo_6Cl_{8-n}S_n^{(4-n)+}$. Because of the demonstrated capacity of α-molybdenum(II)

chloride for undergoing extensive bridging ligand substitution without decomposition, we chose to investigate the substitution of sulfide into this cluster as a potential synthesis for members of the series $Mo_6Cl_{8-n}S_n^{(4-n)+}$.

PART I. SYNTHESIS AND CHARACTERIZATION OF $(C_5H_5NH)_3[(Mo_6Cl_7S)Cl_6]\cdot 3(C_5H_5NH)Cl$ AND $(C_5H_5NH)_3[(Mo_6Cl_7S)Cl_6]$, TWO DERIVATIVES OF THE $(Mo_6Cl_7S)^{3+}$ CLUSTER

INTRODUCTION

The cornerstone of the structures of α-molybdenum(II) chloride and its derivatives is the $Mo_6Cl_8^{4+}$ cluster, which consists of a metal-metal bonded octahedron of molybdenum atoms, with a triply-bridging chloride bound to each face of the octahedron.[19,23] From another viewpoint, the eight bridging chlorides define the vertices of a nonbonded cube, and a molybdenum atom occupies the center of each face of the cube. Each molybdenum atom is also bound to a "terminal" ligand, located on the normal to the cube face. In α-molybdenum(II) chloride, the $(Mo_6Cl_8)Cl_6$ units are linked by sharing of terminal chlorides, as indicated in the formulation $(Mo_6Cl_8)Cl_2Cl_{4/2}$.

The chemistry of α-$MoCl_2$ and its derivatives is consistent with their structure. The labile terminal chlorides can be replaced by a variety of nucleophiles, leaving the robustly bonded $Mo_6Cl_8^{4+}$ cluster untouched.[38,41,42,43] Substitution of the bridging chlorides requires more vigorous reaction conditions.[43,44,45,47] However, the $Mo_6Cl_8^{4+}$ cluster frequently decomposes during attempted substitution of the bridging chlorides.[37,43]

The first example of a halide-chalcide Mo_6X_8 cluster prepared by substitution of sulfide into the bridging chloride sites of $Mo_6Cl_8^{4+}$ is reported. The $Mo_6Cl_7S^{3+}$ cluster has been prepared by a novel route, and isolated in

the 2 compounds $(pyH)_3[(Mo_6Cl_7S)Cl_6]$ and $(pyH)_3[(Mo_6Cl_7S)Cl_6]\cdot 3pyHCl$, where pyH is the pyridinium cation $C_5H_5NH^+$. The crystal and molecular structures of both compounds, and their infrared and chlorine 2p photoelectron spectra are also reported.

EXPERIMENTAL

Materials

Cert. ACS grade pyridine (Fischer Scientific Co.) was vacuum distilled onto outgassed 4A molecular sieves, and vacuum distilled as needed. Cert. ACS grade methanol (Fischer Scientific Co.) and electronic grade hydrochloric acid (Dupont) were used as received. α-Molybdenum(II) chloride was prepared according to the method of Dorman and McCarley.[48] In this procedure, molybdenum(V) chloride is reduced in an aluminum chloride-rich sodium tetrachloroaluminate melt. The molybdenum(II) chloride product is extracted into an ethanol solution. Addition of hydrochloric acid and evaporation of the solution produces crystals of $(H_3O)_2[(Mo_6Cl_8)Cl_6]\cdot 6H_2O$. Heating this product *in vacuo* at 350°C for 24 hours yields pure, anhydrous $(Mo_6Cl_8)Cl_4$. Anhydrous sodium hydrosulfide was prepared by reaction of hydrogen sulfide with sodium ethoxide using the procedure described by Brauer.[49] Both Mo_6Cl_{12} and NaSH were stored in a dry box (dew point *ca.* -75°C).

Syntheses

Preparation of $(pyH)_3[(Mo_6Cl_7S)Cl_6]$

2.00g (2.00mmole) Mo_6Cl_{12} and 0.22g (3.9mmole) NaSH were weighed out in the dry box and transferred to a 250 mL Schlenk reflux flask equipped with a water-cooled condenser.

The flask was transferred to a vacuum line (working vacuum 10^{-4} to 10^{-5} torr), outgassed, and ca. 80 mL of pyridine were distilled onto the reactants. Upon warming to room temperature, vigorous bubbling occurred, and the yellow slurry turned red. The solution was refluxed under a nitrogen atmosphere for 24 hours, and filtered hot under nitrogen. The pyridine was stripped from the red filtrate on the vacuum line, leaving a glassy red solid. In order to remove the unsubstituted $Mo_6Cl_8^{4+}$ cluster, the red solid was stirred for 2 hours at room temperature with ca. 35 mL of a solution of ca. 1M HCl/CH_3OH (3 mL conc. HCl + 33 mL CH_3OH). This slurry was filtered, and the insoluble residue dissolved in 150 mL hot 1M HCl/CH_3OH. The red solution was filtered hot. Dark red crystals of product were obtained by careful evaporation of this filtrate (1.07g, 41% yield). Anal. Calculated for $(C_5H_5NH)_3[(Mo_6Cl_7S)Cl_6]$: Mo, 43.98; Cl, 35.21; S, 2.45; C, 13.76; H, 1.39; N, 3.21; Cl/Mo, 2.17. Found: Mo, 43.50; Cl, 34.57; S, 1.84; C, 12.81; H, 1.45; N, 2.97; Cl/Mo, 2.15.

Preparation of $(pyH)_3[(Mo_6Cl_7S)Cl_6]\cdot 3pyHCl$

The reaction was similar to the one above, until the room temperature wash in HCl/CH_3OH. In the above reaction, a pale yellow solution with insoluble solid resulted from this wash. If 35 mL 2M HCl/CH_3OH, with a few drops of added pyridine is used for the room temperature wash, a pale red

solution (with insoluble residue) results after ca. 2 1/2 hours. 0.58g of beautiful red octahedral crystals of $(pyH)_3[(Mo_6Cl_7S)Cl_6]\cdot 3pyHCl$ was isolated from this solution (18% yield). A small amount of coprecipitated $(pyH)_2[(Mo_6Cl_8)Cl_6]$ (yellow crystals) was separated from the octahedra under the microscope. The insoluble residue from the first washing in HCl/CH_3OH was dissolved in hot HCl/CH_3OH and filtered. 0.41g $(pyH)_3[(Mo_6Cl_7S)Cl_6]$ was subsequently isolated (16% yield). Anal. Calcd. for $(C_5H_5NH)_3[(Mo_6Cl_7S)Cl_6]\cdot 3(C_5H_5NHCl)$: Mo, 34.77; Cl, 34.26; S, 1.94; C, 21.76; H, 2.19; N, 5.07; Cl/Mo, 2.67. Found: Mo, 34.49; Cl, 34.32; S, 1.93; C, 21.49; H, 2.20; N, 4.98; Cl/Mo, 2.69.

Physical Measurements

Chemical analyses

Weighed samples for molybdenum analysis were decomposed by treatment with ammoniacal peroxide solution, heated to dryness, treated with concentrated nitric acid, and again heated to dryness. This decomposition was repeated 2 or 3 times, prior to ignition of the sample to MoO_3. Solutions for chloride and sulfate analysis were prepared by decomposing weighed samples in basic aqueous solutions of sodium peroxide. The solutions were acidified, excess H_2O_2 expelled, and were then ready for analysis. Chloride was determined potentiometrically with a standardized silver nitrate solu-

tion. The sulfur content of $(pyH)_3[(Mo_6Cl_7S)Cl_6]$ was determined gravimetrically as $BaSO_4$. Sulfur in $(pyH)_3[(Mo_6Cl_7S)Cl_6]\cdot 3pyHCl$ was measured by Chemalytics, Inc. Carbon, hydrogen and nitrogen were determined by the Ames Laboratory Analytical Services. Infrared spectra (4000-200 cm^{-1}) were measured as Nujol mulls between CsI plates on a Beckman IR 4250 spectrometer. Reported frequencies are considered accurate to $\pm$ 2 cm^{-1}.

Chlorine 2p photoelectron spectra

Freshly prepared, carefully purified samples were ground in a dry box and spread onto a strip of Ag-Cd alloy. In order to avoid exposure of the fresh surface to air, the sample was transferred directly from the dry box into the AEI ES200B spectrometer. Monochromatic Al Kα radiation (K.E. = 1486.6 eV) was used to irradiate the sample. The electrostatic charge which accumulated at the sample surface during irradiation was maintained at a constant equilibrium value by means of an electron flood gun, which bathed the sample in "zero volt electrons". Good signal to noise ratios resulted when data were accumulated during 400-500 scans over the range of electron binding energies of interest.

The spectral data (number of electron counts for each incremental value of the binding energy within the range recorded) were input to the APES computer program, developed in this laboratory.[50] The program corrects the data, and

then attempts to fit them with a linear combination of Gaussian and Lorentzian functions. The corrections include:

a) two consecutive three (adjacent) point smoothings of the data;

b) a baseline adjustment, so that the minimum number of counts equals zero;

c) a correction for inelastic scattering using the method described by Shirley.[51]

Next, the program calculates a fit to the corrected data, using programmer-supplied values for:

a) the number of component peaks;

b) the approximate energies and heights of the component peaks;

c) the full-width-at-half-maximum (FWHM) of the component peaks.

The energy and height of each component peak are refined by nonlinear least squares during fitting. The FWHM of each peak can also be varied. Constraints can be put on the refinement - e.g., coupling two spin-orbit coupled component peaks (Cl $2p_{1/2}$,$2p_{3/2}$), or requiring equal FWHM for all the component peaks.

The quality of the fit can be assessed from computer-generated plots of calculated and observed spectra, and from χ^2. The physical reasonableness of the refined results must be judged by the program user. In the compounds described

here, the energy separation between spin-orbit coupled peaks and the FWHM of the peaks each fall within a narrow range (see Table VII). The program is particularly helpful if the programmer has a limited number of possible model structures for the compound. Then it can be used to refine the heights of the component peaks in fixed ratios corresponding to the relative ratios of nonequivalent chlorides in the model. The best model corresponds to the best fit.

X-ray Structure Determinations

Collection and reduction of x-ray data for $(pyH)_3[(Mo_6Cl_7S)Cl_6]\cdot 3pyHCl$

$(pyH)_3[(Mo_6Cl_7S)Cl_6]\cdot 3pyHCl$ crystallizes as beautiful red octahedra. The length of the apparent 3-fold axes of the selected crystal was 0.019 cm. All corners of the octahedron were slightly truncated. The crystal was mounted with a 3-fold axis approximately collinear with Φ on an automated 4 circle diffractometer.[52] Eight reflections were selected from ω-oscillation photographs taken at Φ=0°, 30°, 60°, 90°. The angular coordinates of the eight reflections were input to the automatic indexing program ALICE,[53] which calculated the orientation matrix, the reduced unit cell, and the reduced cell scalars. These approximate cell parameters and the scalars indicated cubic crystal symmetry.

During data collection, a periodic check of the intensities of the three standard reflections (after every 75 reflections) indicated no significant crystal or instrument instability. Accurate unit cell parameters and their estimated standard deviations were determined by a least squares fit to the $\pm 2\theta$ values of twelve independent high angle ($2\theta \geq 30°$) reflections.

The intensity data were then corrected for Lorentz polarization effects. An absorption correction was not necessary. Except for weakly observed reflections that were discarded because less than half of their symmetry-related reflections were observed, all equivalent data were averaged.

Solution and refinement of the structure

816 independent reflections were used in the structure refinement. The 0kl reflections with l=2n+1 were systematically unobserved. In order that the structure could be refined in the space group Pa3, the k and l indices of all reflections were interchanged, and the signs of the new k indices changed.

The position of the molybdenum atom was located using Patterson superposition techniques.[54] The bridging ligand, ionic and terminal chloride positions were determined from subsequent electron density maps.[55] (Note: Because of the very similar x-ray scattering power of Cl and S, we were

unable to ascertain whether S is localized on one of the two independent sets of bridging ligand sites of the $Mo_6Cl_7S^{3+}$ cluster or disordered over both. The scattering factor of Cl was used in the refinement of both sets of bridging ligand parameters.) Following refinement of the positional and isotropic thermal parameters of these atoms, the discrepancy factor ($R=\Sigma||F_o|-|F_c||/\Sigma|F_o|$) was 0.189. The six atom positions defining the pyridinium cation were determined from sharpened electron density difference maps.[56] Because these six positions could not be distinguished, they were refined using an averaged scattering factor (1/6 N, 5/6 C). At this point, problems were encountered in the refinement of all twelve atoms, due to severe overshifting of the constrained X(1) and Cl,i positional parameters (both on c sites with 3 site symmetry). The refinement of these positions, and subsequently of the anistropic thermal parameters of these atoms and of Cl,is (a site, $\bar{3}$ site symmetry) were damped by using half shifts. Prior to anisotropic refinement of the pyridinium cation, its hydrogen atom positions were calculated and input, but not refined. The positions and anisotropic thermal parameters of all nonhydrogen atoms were refined by full matrix least squares techniques,[56] using the scattering factors of Hanson et al.,[57] with molybdenum and chlorine corrected for the real and

imaginary parts of anomalous dispersion.[58] There was no significant electron density (>1e/Å^3) in the final electron density difference map.

Collection and reduction of x-ray data for $(pyH)_3[Mo_6Cl_7S)Cl_6]$

This compound crystallizes in the form of dark red cubes. A number of these crystals was checked, and all were twinned. An irregularly shaped crystal chip (not a twin) of dimensions 0.026 x 0.017 x 0.010 cm was chosen for the structure determination. Crystal indexing indicated a monoclinic unit cell. Data collection proceeded as before.[52] Since a slight decrease in the standards' intensities occurred, a scaling procedure was used to normalize the raw data. The intensity data were corrected for Lorentz polarization effects. Although several attempts were made to correct the data for absorption with the Tompa Alcock program, none of the corrected data sets refined as well as the uncorrected one. Calculated transmission factors ranged from 0.68 to 0.83. Equivalent reflections were averaged; the criterion for inclusion in the data set was $(|F_o| - |F_a|)/|F_a| \leq 0.20$.

Solution and refinement of the structure

3347 independent reflections were used in the structure refinement. The h01 with l=2n+1 and 0k0 with k=2n+1

reflections were systematically absent, indicating the $P2_1/c$ space group. The molybdenum, bridging and terminal ligand positions were located as before. (Note: Because we were also unable to ascertain the disposition of S over the bridging ligand sites of this $(Mo_6Cl_7S)^{3+}$ cluster, the bridging ligand parameters were again refined using the scattering factor of chlorine). Refinement of the positions and isotropic thermal parameters of these atoms resulted in a discrepancy factor of 0.149. The carbon and nitrogen positions of the pyridinium cations were located in sharpened electron density difference maps.[56] Because the distinction between N and C atoms was not checked during final stages of the structure refinement (as it was in the case of $(pyH)_3[(Mo_6Cl_7S)Cl_6]\cdot 3pyHCl$), this distinction is tentative, i.e., the nitrogen may again be disordered over all 6 sites of each ring. Subsequent refinement proceeded smoothly. All atoms except for carbon and nitrogen were refined anisotropically by full matrix least squares techniques.[56] Because of the large thermal parameters of the carbon and nitrogen atoms, they were refined isotropically. There was no significant electron density in the final electron density difference map.[55] Final positional and thermal parameters of the two structures are listed in Tables II-V. Tables of observed and calculated structure factors are available as supplementary material.

Table I. Summary of crystal data, intensity collection, and structure refinement

compound	$(C_5H_5NH)_3[(Mo_6Cl_7S)Cl_6]\cdot 3(C_5H_5NH)Cl$	$(C_5H_5NH)_3[(Mo_6Cl_7S)Cl_6]$
formula weight	1655.61	1308.92
space group	Pa3	$P2_1/c$
a (Å)	17.158(2)	13.469(4)
b (Å)		15.329(3)
c (Å)		17.112(5)
β (deg)		107.19(3)
Z	4	4
ρ_{calc} (g cm^{-3})	2.18	2.58
ρ_{obs} (g cm^{-3})	2.18 (flotation in 1,2-$C_2H_4Br_2$)	2.6(flotation)
μ (cm^{-1})	23.3	32.0
no. refl. to detn. cell constants	12	17
λ(Mo Kα,Å)	0.70954	0.70954
monochromator	graphite crystal	graphite crystal
takeoff angle (deg)	4.5	4.5
2θ limit (deg)	50	45
octants measured	h,k,l	h, ±k, ±l
no. standard refl.	3	3
function minimized	$\Sigma w(\|Fo\|-\|F_c\|)^2$, $w=1/\sigma_F^2$	$\Sigma w(\|F_o\|-\|F_c\|)^2$
R	0.054	0.063
R_w	0.058	0.074

Table II. Final positional parameters for $(C_5H_5NH)_3[(Mo_6Cl_7S)Cl_6]\cdot 3(C_5H_5NH)Cl$[a]

Atom	x	y	z
Mo	0.47921(6)	0.52633(6)	0.60219(6)
X(1)	0.6019(5)	0.6019(5)	0.6019(5)
X(2)	0.5518(2)	0.4082(2)	0.6415(2)
Cl	0.4535(2)	0.5615(2)	0.7386(2)
Cl,i	0.1923(8)	0.1923(8)	0.1923(8)
Cl,is	0	0	0
R(1)	0.186(2)	0.246(2)	0.877(1)
R(2)	0.235(1)	0.244(1)	0.932(2)
R(3)	0.230(1)	0.192(2)	0.992(1)
R(4)	0.174(2)	0.138(1)	0.989(2)
R(5)	0.123(1)	0.140(1)	0.932(3)
R(6)	0.130(2)	0.196(2)	0.874(2)
H(1)	0.19	0.29	0.83
H(2)	0.29	0.29	0.94
H(3)	0.27	0.19	1.04
H(4)	0.17	0.09	1.04
H(5)	0.08	0.10	0.93
H(6)	0.09	0.19	0.83

[a]Numbers in parentheses are the estimated standard deviations of the coordinates and refer to the last significant digit of the preceding number.

Table III. Final positional parameters for $(C_5H_5NH)_3[(Mo_6Cl_7S)Cl_6]$[a]

Atom	x	y	z
Mo(1c)	0.87359(9)	0.94560(8)	0.48487(8)
Mo(2c)	1.04372(9)	0.95781(8)	0.60558(7)
Mo(3c)	0.94890(9)	1.09809(8)	0.53659(7)
Mo(1b)	0.52761(9)	0.39983(8)	0.45126(7)
Mo(2b)	0.53451(9)	0.44436(8)	0.59942(7)
Mo(3b)	0.36381(9)	0.46521(8)	0.48109(7)
X(1c)	0.8735(3)	0.0018(3)	0.6190(2)
X(2c)	0.9700(3)	0.8147(2)	0.5505(2)
X(3c)	0.1138(3)	0.1042(2)	0.6505(2)
X(4c)	0.7895(3)	1.0818(2)	0.4198(2)
X(1b)	0.4295(3)	0.3188(2)	0.5302(2)
X(2b)	0.6884(3)	0.3849(2)	0.5664(2)
X(3b)	0.3783(3)	0.5098(3)	0.6220(2)
X(4b)	0.3640(3)	0.4255(2)	0.3399(2)
Cl(1c)	0.7062(3)	0.8730(3)	0.4660(3)
Cl(2c)	1.0999(3)	0.9049(3)	0.7470(2)
Cl(3c)	0.8811(3)	1.2293(3)	0.5848(3)
Cl(1b)	0.5637(4)	0.2619(3)	0.3912(3)
Cl(2b)	0.5809(3)	0.3675(3)	0.7308(2)
Cl(3b)	0.1837(3)	0.4155(3)	0.4570(3)
N(1)	0.531(2)	0.386(2)	0.183(1)
C(1)	0.589(2)	0.337(2)	0.149(2)
C(2)	0.626(2)	0.386(2)	0.091(2)
C(3)	0.608(2)	0.479(2)	0.082(2)
C(4)	0.541(3)	0.521(2)	0.124(2)
C(5)	0.509(2)	0.474(2)	0.171(2)

[a]Numbers in parentheses are the estimated standard deviations of the coordinates and refer to the last significant digit of the preceding number.

Table III. (continued)

Atom	x	y	z
N(2)	0.202(2)	0.716(2)	0.688(1)
C(6)	0.122(2)	0.672(2)	0.725(2)
C(7)	0.066(2)	0.598(2)	0.682(2)
C(8)	0.085(2)	0.574(2)	0.613(2)
C(9)	0.149(2)	0.616(2)	0.579(2)
C(10)	0.202(2)	0.681(2)	0.616(2)
N(3)	0.885(2)	0.820(1)	0.770(1)
C(11)	0.806(2)	0.800(2)	0.695(2)
C(12)	0.707(2)	0.792(2)	0.704(2)
C(13)	0.689(2)	0.800(2)	0.775(1)
C(14)	0.768(2)	0.818(2)	0.844(1)
C(15)	0.867(2)	0.831(2)	0.840(2)

Table IV. Final thermal parameters ($\times 10^3$) for $(C_5H_5NH)_3[(Mo_6Cl_7S)Cl_6]\cdot 3(C_5H_5NH)Cl$[a]

Atom	β_{11}	β_{22}	β_{33}	β_{12}	β_{13}	β_{23}
Mo	3.33(5)	3.50(5)	3.13(5)	-0.07(4)	0.07(4)	-0.09(4)
X(1)	3.7(3)	3.7(3)	3.7(3)	-0.2(3)	-0.2(3)	-0.2(3)
X(2)	4.5(1)	4.0(1)	3.7(1)	0.0(1)	-0.4(1)	0.6(1)
Cl	5.9(2)	5.9(2)	3.5(1)	-0.5(1)	0.5(1)	-0.5(1)
Cl,i	8.8(7)	8.8(7)	8.8(7)	-1.5(6)	-1.5(6)	-1.5(6)
Cl,is	8.6(9)	8.6(9)	8.6(9)	0.2(10)	0.2(10)	0.2(10)
R(1)	10(2)	9(1)	5(1)	4(1)	0(1)	1(1)
R(2)	8(1)	4(1)	15(2)	-1(1)	2(1)	1(1)
R(3)	9(1)	7(1)	8(1)	3(1)	-3(1)	-1(1)
R(4)	12(2)	5(1)	8(1)	1(1)	4(1)	2(1)
R(5)	6(1)	6(1)	15(2)	-1(1)	0(1)	-4(1)
R(6)	9(2)	10(2)	9(1)	1(1)	-3(1)	-4(1)

[a]The form of the anisotropic temperature factor expression is $\exp[-(\beta_{11}h^2+\beta_{22}k^2+\beta_{33}\ell^2+2\beta_{12}hk+2\beta_{13}h\ell+2\beta_{23}k\ell)]$.

Table V. Final thermal parameters for $(C_5H_5NH)_3[(Mo_6Cl_7S)Cl_6]$[a]

Atom	β_{11}	β_{22}	β_{33}	β_{12}	β_{13}	β_{23}
Mo(1c)	35.4(8)	31.9(6)	32.6(6)	-0.3(6)	10.7(5)	1.2(4)
Mo(2c)	41.8(8)	34.3(6)	28.2(5)	1.2(6)	10.4(6)	1.9(4)
Mo(3c)	39.4(8)	29.6(6)	32.6(6)	3.6(6)	12.6(6)	-0.8(4)
Mo(1b)	41.9(8)	30.6(6)	27.7(5)	1.9(6)	11.6(5)	-3.9(4)
Mo(2b)	38.4(8)	33.1(6)	24.8(5)	1.0(6)	10.8(5)	3.2(4)
Mo(3b)	32.2(8)	34.6(6)	29.2(5)	-0.9(6)	10.0(5)	1.1(4)
X(1c)	61(3)	50(2)	42(2)	2(2)	22(2)	1(2)
X(2c)	53(3)	34(2)	45(2)	1(2)	15(2)	7(1)
X(3c)	58(3)	43(2)	37(2)	-6(2)	8(2)	-6(1)
X(4c)	43(2)	41(2)	42(2)	7(2)	6(2)	5(1)
X(1b)	57(3)	33(2)	42(2)	-7(2)	13(2)	3(1)
X(2b)	43(2)	43(2)	40(2)	10(2)	12(2)	5(1)
X(3b)	57(3)	53(2)	36(2)	3(2)	22(2)	2(2)
X(4b)	56(3)	45(2)	31(2)	-4(2)	5(2)	-5(1)
Cl(1c)	49(3)	55(2)	72(3)	-14(2)	17(2)	3(2)
Cl(2c)	75(3)	77(3)	34(2)	4(2)	11(2)	13(2)
Cl(3c)	79(3)	45(2)	59(2)	17(2)	27(2)	-5(2)
Cl(1b)	90(4)	49(2)	63(2)	6(2)	24(2)	-23(2)
Cl(2b)	75(3)	66(2)	34(2)	11(2)	14(2)	18(2)
Cl(3b)	41(3)	80(3)	68(3)	-16(2)	11(2)	10(2)

N(1)[b]	11.6(7)
C(1)	10.5(7)
C(2)	10.6(7)
C(3)	11.0(8)
C(4)	12.0(9)
C(5)	9.2(6)
N(2)	10.9(6)
C(6)	9.4(6)
C(7)	9.6(7)
C(8)	9.9(7)
C(9)	11.3(8)
C(10)	8.4(6)
N(3)	10.3(6)
C(11)	10.0(7)
C(12)	9.3(6)
C(13)	8.1(6)
C(14)	8.8(6)
C(15)	8.9(6)

[a]The form of the anisotropic temperature factor expression is $\exp[-(\beta_{11}h^2+\beta 22k^2+\beta_{33}\ell^2+2\beta_{12}hk+2\beta_{13}h\ell+2\beta_{23}k\ell)]$. Values of β_{ij} are $x10^4$.

[b]The form of the isotropic temperature factor expression is $\exp[-\beta(\sin^2\theta/\lambda^2)]$.

DISCUSSION OF RESULTS

Syntheses

Substitution at the bridging chloride sites of the $Mo_6Cl_8^{4+}$ cluster requires vigorous reaction conditions. If the attacking ligand is bromide or iodide, complete substitution proceeds smoothly, yielding the stable $Mo_6X_8^{4+}$ (X=Br,I) clusters.[44] However, substitution by nonhalides frequently causes cluster decomposition, due to the instability of the desired products toward degradative oxidation. No more than two hydroxides can be substituted into the bridging chloride sites of $Mo_6Cl_8^{4+}$ before cluster degradation occurs.[43,46] The cluster is more tolerant toward substitution by methoxide. Complete substitution is possible, but the resulting compound, $Na_2[(Mo_6(OCH_3)_8)(OCH_3)_6]$, is pyrophoric.[47]

The $Mo_6Cl_7S^{3+}$ cluster is the first example of a halide-chalcide M_6X_8 cluster prepared by substitution of chalcide into the $Mo_6Cl_8^{4+}$ cluster. This substitution is not hindered by product instability. Crystals of both compounds in which the $Mo_6Cl_7S^{3+}$ cluster has been isolated are indefinitely stable in air; solutions in acetonitrile or CH_3OH/HCl are slowly (weeks) oxidized. More extensively substituted sulfide derivatives of $Mo_6Cl_8^{4+}$ exhibit similar stability, and are also accessible via this novel preparation.[59]

The first step of the preparation is the reaction between α-molybdenum(II) chloride and sodium hydrosulfide in pyridine. Dissolution of the highly reactive, amorphous $(Mo_6Cl_8)Cl_4$ causes vigorous bubbling. A flocculent, brilliant red precipitate forms before the reaction reaches reflux temperature. Although this solid has not been identified, reacting it with HCl/CH_3OH yields $(pyH)_2[(Mo_6Cl_8)Cl_6]$, strong evidence that it contains the untouched $Mo_6Cl_8^{4+}$ cluster, with sulfide in some of the terminal ligand sites. Substitution of sulfide into a bridging ligand site is achieved by refluxing the reaction mixture 24 hours. A filtration to remove NaCl and other insoluble products follows. By careful evaporation, a few poorly formed crystals have occasionally been isolated from the filtrate; however, the product is generally isolated as a glassy red solid by removing all the solvent. The infrared spectrum of the solid consists of bands assigned either to vibrations of coordinated pyridine[60] or to Mo-Cl vibrations. The optimum yield of the $Mo_6Cl_7S^{3+}$ cluster (isolated after the reaction with HCl) is obtained using the proportions:

$$(Mo_6Cl_8)Cl_4 + 2NaSH \xrightarrow{py} "(Mo_6Cl_7S)Cl_3py_3" + 2NaCl + pyHSH.$$

Subsequent reaction with HCl yields the final product:

$$"(Mo_6Cl_7S)Cl_3py_3" + 3HCl \longrightarrow (pyH)_3[(Mo_6Cl_7S)Cl_6].$$

Depending on the concentrations of Cl^- and pyH^+ in the solution, this salt is isolated neat, or with 3 formula units of pyHCl in the lattice.

Physical Measurements

The physical techniques used to characterize these two compounds complement each other beautifully in the determination of their structures and compositions. The x-ray structure determinations indicated the structures of the 2 formula units $(pyH)_3[(Mo_6X_8)X_6]$ and $(pyH)_3[(Mo_6X_8)X_6]\cdot 3pyHCl$. The analytical data agree quite well with the respective formulations $(pyH)_3(Mo_6Cl_{13}S)$ and $(pyH)_6(Mo_6Cl_{16}S)$. At this stage, despite chemical evidence indicating sulfide occupied a bridging ligand site (i.e., reaction with HCl had not regenerated $(Mo_6Cl_8)Cl_6^{2-}$), the question of whether sulfide occupied a bridging or terminal ligand site was still moot. The chlorine 2p photoelectron spectra indicate unambiguously that the sulfide in both compounds is in a bridging ligand site; thus, the 2 compounds are $(pyH)_3[(Mo_6Cl_7S)Cl_6]$ and $(pyH)_3[(Mo_6Cl_7S)Cl_6]\cdot 3pyHCl$. The infrared spectra of both compounds are identical in the

200-450 cm^{-1} region, good evidence that $(Mo_6Cl_7S)Cl_6^{3-}$ is the cluster species in both compounds.

Finally, there is little question that the sulfides are deprotonated. A triply bridging SH^- ligand is unknown, presumably because it is quite acidic. The absence of an electron spin resonance signal for either compound leaves very little doubt about the matter; if the sulfide were protonated, both compounds would have an odd number of electrons.

Infrared spectra

The infrared spectra of the two compounds are practically identical; some bands assigned to the pyridinium cation[60] are more intense in the spectrum of $(pyH)_3[(Mo_6Cl_7S)Cl_6]\cdot 3pyHCl$. The equivalence of the spectra in the Mo-Cl stretching region confirms that the $(Mo_6Cl_7S)Cl_6^{3-}$ unit is present in both compounds. Predictably, the pattern of the bands in this region is quite similar to that of $(Mo_6Cl_8)Cl_6^{2-}$. However, inspection of Table VI demonstrates that band locations and intensities in the spectra of the $(Mo_6Cl_7S)Cl_6^{3-}$ and $(Mo_6Cl_8)Cl_6^{2-}$ clusters are significantly different. Also, a new band appears in the spectrum of $(Mo_6Cl_7S)Cl_6^{3-}$ at 421 cm^{-1}. This band has not been observed in the spectra of other pyridinium salts, and its frequency is too high for a Mo(II)-Cl vibration of a hexanuclear

Table VI. Low frequency infrared data (200-450 cm^{-1})[a]

$(C_5H_5NH)_3[(Mo_6Cl_7S)Cl_6]$	$(C_5H_5NH)_3[(Mo_6Cl_7S)Cl_6]\cdot 3(C_5H_5NH)Cl$	$[(n\text{-}C_4H_9)_4N]_2[(Mo_6Cl_8)Cl_6]$	$(C_5H_5NH)_2[(Mo_6Cl_8)Cl_6]$
421 m-s	423 m		
389 w	390 m	388 vw	390 vw
		376 vw	
362 w		355 sh	355 w,sh
	344 w		
312 vs	310 vs	325 vs	321 vs
	271 vw,sh	271 vw,sh	266 vw
230 s	230 m-s	237 s	236 vs
218 sh	213 sh	214 w-m	209 m

[a]Spectra obtained from Nujol mulls. Abbreviations: s, strong; m, medium; w, weak; v, very; sh, shoulder.

cluster.[61] Thus, it is unique to the $(Mo_6Cl_7S)Cl_6^{3-}$ cluster unit. Caution must be exercised in assigning this band, since Hogue and McCarley have shown that extensive mixing of the normal vibrational modes of M_6X_8 clusters occurs.[62] Thus, since the 421 cm^{-1} band undoubtedly mixes with the other modes of the $(Mo_6Cl_7S)Cl_6^{3-}$ cluster, it is assigned to a vibration of predominant (Mo-S) character. The high frequency of this vibration is not unreasonable when compared to the frequency of the (Mo_3S) vibration (459 cm^{-1}) of the $[Mo_3(\mu_3\text{-}S)(\mu_2\text{-}S_2)_3]^{2-}$ cluster.[63]

Chlorine 2p photoelectron spectra

X-ray photoelectron spectroscopy (PES) has been developed into an important tool for the structural characterization of transition metal halides.[64,65] Because the binding energy of the core level electrons of an atom are sensitive to its chemical environment, PES can be used to determine the number of different "types" of halide (triply-bridging, terminal, etc.) in a metal halide. Hamer and Walton have demonstrated that α-molybdenum(II) chloride and its derivatives are a particularly favorable case because of a large binding energy difference between the triply-bridging and terminal chlorides in these compounds of ca. 2.3 eV.[66] Thus, although the Cl 2p photoelectron spectra are complicated by spin-orbit coupling (each type of chloride has 2 spin-orbit coupled peaks, with a

binding energy separation of ca. 1.5 eV), the spectra of these compounds can be resolved into component peaks, and the ratio of the number of bridging to the number of terminal chlorides (Cl_b/Cl_t) derived.

The calculated and observed Cl 2p photoelectron spectra of 3 compounds are shown in Figure 3. An excellent fit was achieved for the spectrum of $[(n\text{-}C_4H_9)_4N]_2[(Mo_6Cl_8)Cl_6]$, with a ratio Cl_b/Cl_t=1.43 (8/6=1.33 is the correct value). A similarly shaped spectrum is obtained for $(pyH)_3[(Mo_6Cl_7S)Cl_6]$. An excellent fit was obtained with a ratio Cl_b/Cl_t=1.12. Any remaining ambiguity in the location of sulfide in the $Mo_6Cl_{13}S^{3-}$ cluster is dispelled; of the two possible models, $(Mo_6Cl_7S)Cl_6^{3-}$ (expected ratio Cl_b/Cl_t=1.17) and $(Mo_6Cl_8)SCl_5^{3-}$ (expected ratio Cl_b/Cl_t=1.60), the first is obviously the correct one.

The appearance of the spectrum of $(pyH)_3[(Mo_6Cl_7S)Cl_6]\cdot$ 3pyHCl differs because there are three types of chloride in this compound. Prior to the solution of the x-ray crystal structure, we determined that this compound probably had 3 types of chloride, because we were unable to fit the observed spectrum with only 2 types. The calculated spectrum shown in Figure 3 was obtained by fixing the ratio $Cl_b/Cl_t/Cl_i$ at the correct value ($7Cl_b:6Cl_t:3Cl_i$). A better fit was obtained without this constraint, but was not physically reasonable. Of the reasonable models, this correct model gave the best fit.

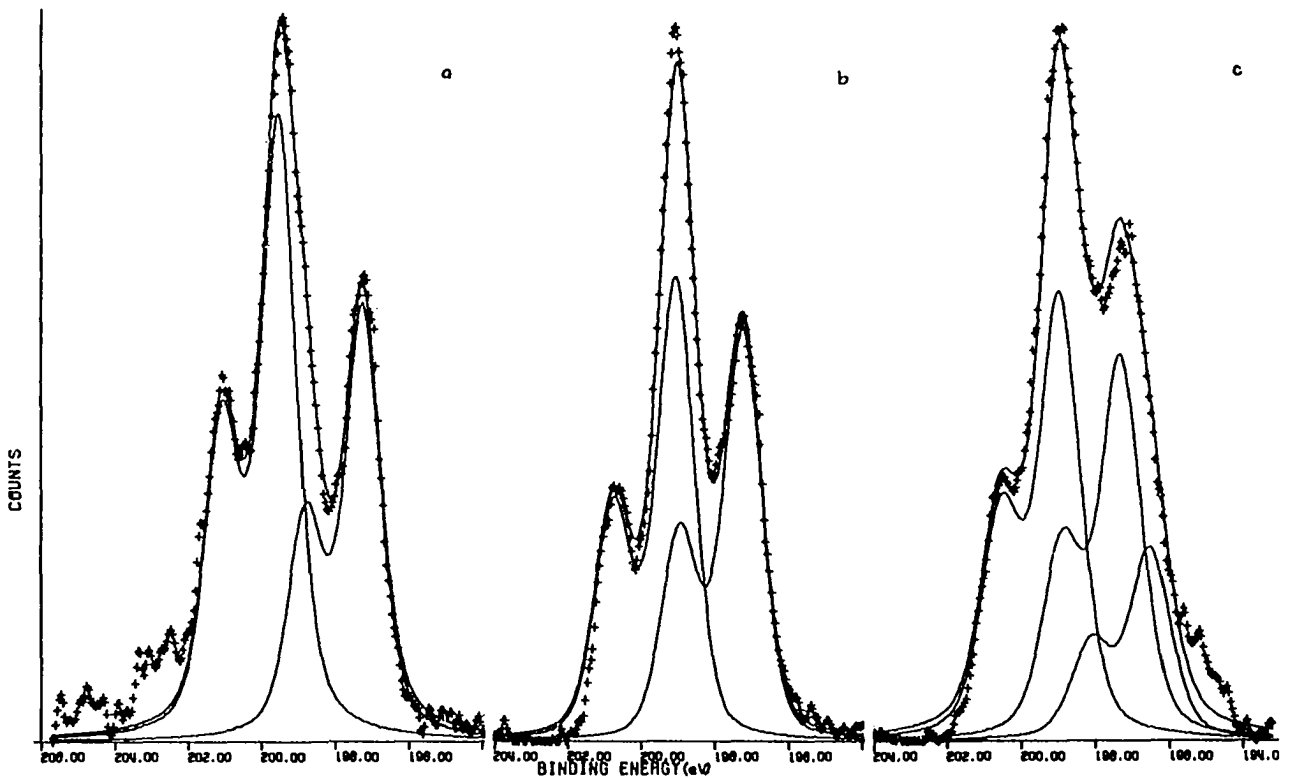

Figure 3. The chlorine 2p photoelectron spectra of $[(n\text{-}C_4Hg)_4N]_2[(Mo_6Cl_8)Cl_6]$, a; $(C_5H_5NH)_3[(Mo_6Cl_7S)Cl_6]$, b; $(C_5H_5NH)_3[(Mo_6Cl_7S)Cl_6]\cdot 3(C_5H_5NH)Cl$, c

Table VII lists data derived from these calculated spectra, along with corresponding data for 2 other salts of $[(Mo_6Cl_8)Cl_6]^{2-}$. Although the same referencing procedure was used to determine the binding energies in these two $(Mo_6Cl_8)Cl_6^{2-}$ salts, corresponding binding energies differ by 0.4-0.5 eV. However, the difference in binding energy between the bridging and terminal chlorides (the binding energy "shift") is nearly identical in all three $(Mo_6Cl_8)Cl_6^{2-}$ salts. Thus, although comparison of corresponding binding energies in a series of compounds is risky, comparisons of binding energy shifts are quite valid.

As expected, corresponding binding energies of the two $(Mo_6Cl_7S)Cl_6^{3-}$ salts agree within 0.1 eV. Surprisingly, the binding energy shift in the $(Mo_6Cl_7S)Cl_6^{3-}$ cluster has dropped to 1.7-1.8 eV, 0.5 eV smaller than the shift observed in the isostructural, isoelectronic $(Mo_6Cl_8)Cl_6^{2-}$ cluster, or any of the other derivatives of α-molybdenum(II) chloride.[66] The shift in $(Mo_6Cl_7S)Cl_6^{3-}$ is quite comparable to the binding energy shift of 1.8-1.9 eV between <u>doubly</u>-bridging and terminal chlorides of $(Nb_6Cl_{12})Cl_2\ L_4$ ($L=(CH_3)_2SO$, $P(n\text{-}C_3H_7)_3$) and $[(C_2H_5)_4N]_3[(Nb_6Cl_{12})Cl_6]$.[67] No reason for the anomalously small shift in $(Mo_6Cl_7S)Cl_6^{3-}$ can be found in its structure; indeed, the bond distances (vide infra) indicate the bridging chlorides are bound as strongly as in α-molybdenum(II) chloride, the terminal ligands not as strongly bound, leading

Table VII. Chlorine 2p photoelectron data

Compound	Cl $2p_{3/2}$ Binding Energies (eV)[a]			FWHM[b] (eV)	ESSO[b] (eV)	Reference
	bridging	terminal	ionic			
$((n\text{-}C_4H_9)_4N)_2[(Mo_6Cl_8)Cl_6]$	199.4	197.2		1.14	1.55	this work
$(C_5H_5NH)_3[(Mo_6Cl_7S)Cl_6]$	199.0	197.2		1.20	1.70	this work
$(C_5H_5NH)_3[(Mo_6Cl_7S)Cl_6]\cdot 3(C_5H_5NH)Cl$	198.9	197.2	196.4	1.30	1.60	this work
$((C_2H_5)_4N)_2[(Mo_6Cl_8)Cl_6]$[c]	200.1	197.8			1.6,1.6	66
$(H_3O)_2[(Mo_6Cl_8)Cl_6]$[c]	199.6	197.4			1.6,1.4	66

[a]Unless noted otherwise, the reference for all binding energy data is the C 1s binding energy (284.0 eV) of the cation.

[b]Abbreviations: FWHM, full-width-at-half-maximum; ESSO, energy separation between spin-orbit coupled peaks.

[c]Reference is C 1s binding energy (284.0 eV) of graphite contaminant.

one to expect a slightly larger shift in $(Mo_6Cl_7S)Cl_6^{3-}$. An explanation of the anomalous binding energy shift of $(Mo_6Cl_7S)Cl_6^{3-}$ will be deferred until a definite trend can be established from the data of other sulfur-substituted clusters.

The binding energy shift between the terminal and ionic chlorides of $(pyH)_3[(Mo_6Cl_7S)Cl_6]\cdot 3pyHCl$ is 0.8 eV, halfway between the 1.6 eV Cl_t-Cl_i shifts in octahedral $(ML_2Cl_2)Cl$ complexes (M=Cr(III), Rh(III); L=2,2'-bipyridine, 2,5-dithiahexane, 1,2-bis(diphenylphosphino)ethane, 1,2-bis(diphenylarsino)ethane) and the 0 eV shift in the analogous amine (L=NH_3, ethylenediamine) complexes.[68] Ebner et al. speculated that the binding energy of the ionic chloride in the amine complexes had been increased by N-H---Cl hydrogen bonding interactions, causing a decreased shift. Hydrogen bonding between the pyridinium cations and ionic chlorides of $(pyH)_3[(Mo_6Cl_7S)Cl_6]\cdot 3pyHCl$ may have a similar, but apparently smaller effect. On the other hand, the intermediate value of the Cl_t-Cl_i shift of $(pyH)_3[(Mo_6Cl_7S)Cl_6]\cdot 3pyHCl$ may reflect weaker metal-Cl_t bonding in the cluster than in the monomeric complexes. However, the metal-Cl_t bond strengths in the cluster and in the complexes are not readily compared, due to the dissimilarity of these two types of compounds.

X-ray Structure Determinations

The structure of $(pyH)_3[(Mo_6Cl_7S)Cl_6]\cdot 3pyHCl$ consists of $(Mo_6Cl_7S)Cl_6^{3-}$ clusters located halfway along the edges and at the body center of the unit cell (b site, $\bar{3}$ site symmetry), chloride ions (Cl,is) at the origin and face centers of the unit cell (b site, $\bar{3}$ site symmetry), 8 more chloride ions (Cl,i) within the unit cell (c site, 3 site symmetry), and 24 pyridinium cations in general cell positions. For clarity, separate views of the chloride ions and clusters (Figure 4) and of the pyridinium cations (Fig. 5) are presented.[69] The nearest neighbors of both types of chloride ions are the pyridinium cations. There are 3 (Cl,i)-R1 contacts of 3.35(3)Å, and 6 (Cl,is)-R5 contacts of 3.40(3)Å. (Note: Since the six nonhydrogen atoms of the pyridinium cation were indistinguishable, they were labelled R1-R6). Since the sum of the van der Waals radii of nitrogen and chlorine is 3.30-3.45Å, these contacts may be weak hydrogen bonds.[70] Neither Cl,i nor Cl,is has any other neighbors (excluding pyridinium hydrogens) closer than 3.5Å. There is no significant contact (<3.5Å) of the cluster with the pyridinium cation.

In the structure of $(pyH)_3[(Mo_6Cl_7S)Cl_6]$, the $(Mo_6Cl_7S)Cl_6^{3-}$ clusters again occupy the edge centers and body center of the unit cell (b and c sites, $\bar{1}$ site symmetry),

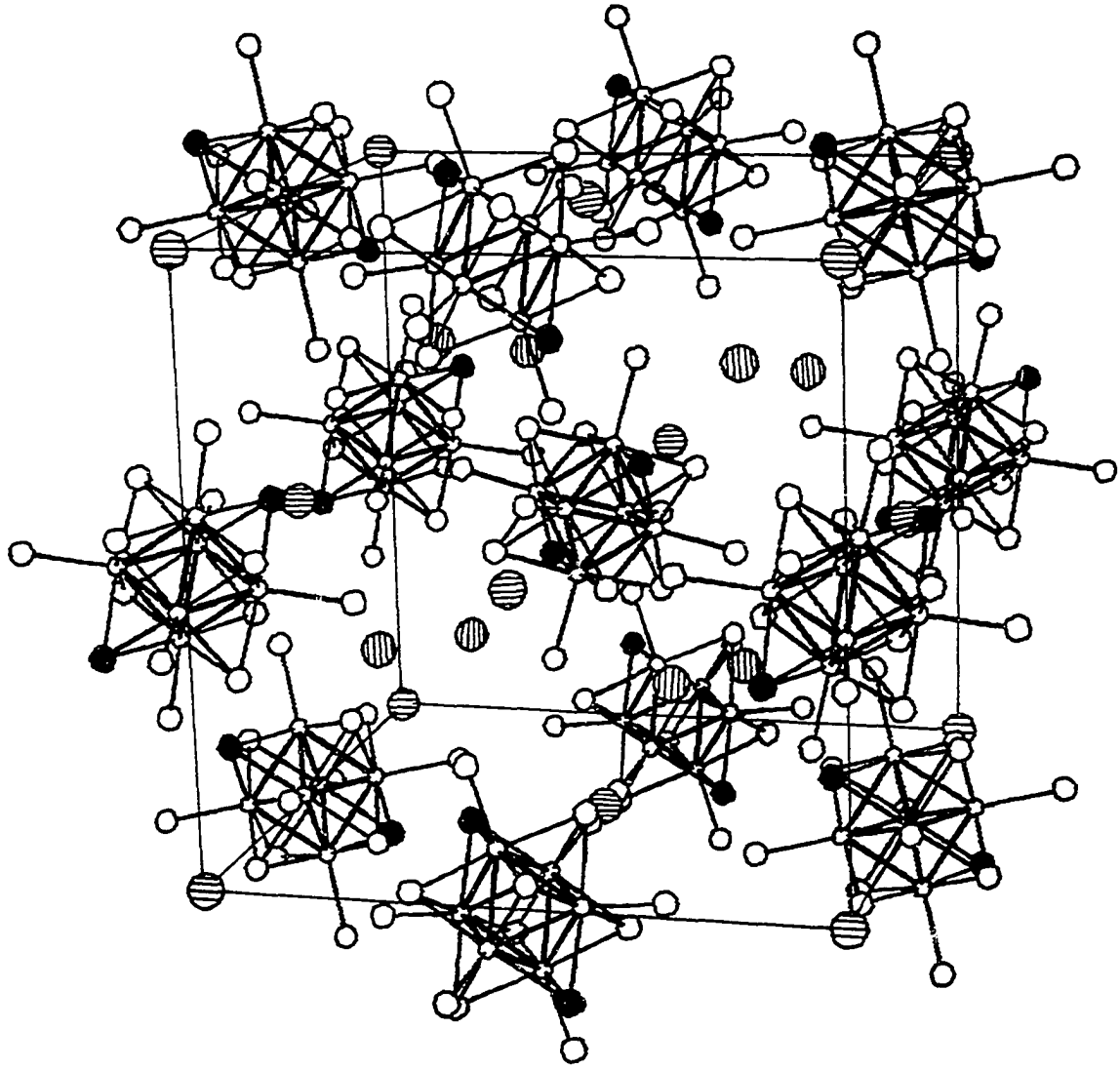

Figure 4. A perspective view of the $(Mo_6Cl_7S)Cl_6^{3-}$ clusters (darkened atoms lie on cluster's 3-fold axis) and chloride ions (crosshatched atoms) in the unit cell of $(C_5H_5NH)_3[(Mo_6Cl_7S)Cl_6]\cdot 3(C_5H_5NH)Cl$

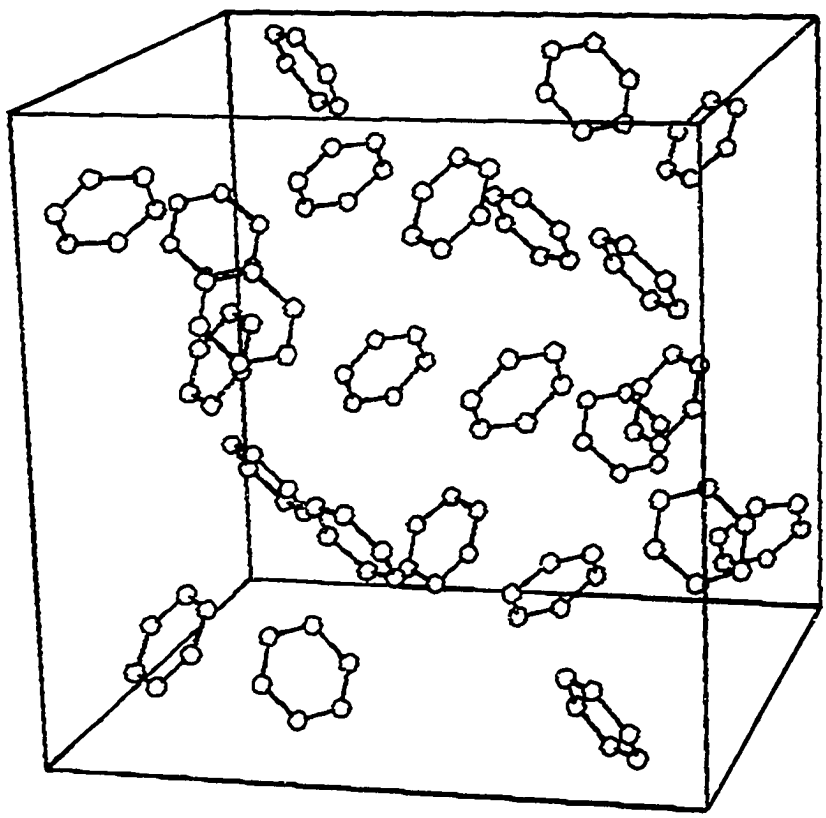

Figure 5. A perspective view of the pyridinium cations in the unit cell of $(C_5H_5NH)_3[(Mo_6Cl_7S)Cl_6]\cdot 3(C_5H_5NH)Cl$

and the twelve pyridinium cations occupy general cell positions. The clusters on the b and c sites are crystallographically independent. The clusters in this structure have several contacts with the pyridinium cations which are noticeably shorter than 3.45Å. One of the bridging ligands (X3b) is 3.38(3)Å from C9 and 3.43(3)Å from C5. Two of the terminal chlorides of each cluster (Cl2c, Cl1b) are 3.31(3)Å from a carbon atom and 2 more terminal chlorides of each cluster (Cl3c, Cl2b) are 3.37-3.38(3)Å from other carbon atoms. However, these contacts are not smaller than the sum of the van der Waals radii. Although weak hydrogen bonding may be involved, the close similarity of the bond distances and angles within these two clusters to those in the cluster of $(pyH)_3[(Mo_6Cl_7S)Cl_6]\cdot 3pyHCl$ indicates the closer pyridinium-cluster contacts in $(pyH)_3[(Mo_6Cl_7S)Cl_6]$ have no significant effect on the intracluster bonding.

The $(Mo_6Cl_7S)Cl_6^{3-}$ cluster of $(pyH)_3[(Mo_6Cl_7S)Cl_6]\cdot 3pyHCl$ is illustrated in Figure 6. The structure of this cluster is indistinguishable from that of a derivative of Mo_6Cl_{12}, with an octahedron of metal-metal bonded molybdenum atoms, 8 bridging ligands, and 6 terminal chlorides. The labels used in Figure 6 correspond to atom labels used for the interatomic distances and angles of both compounds listed in Tables VIII-X.[71]

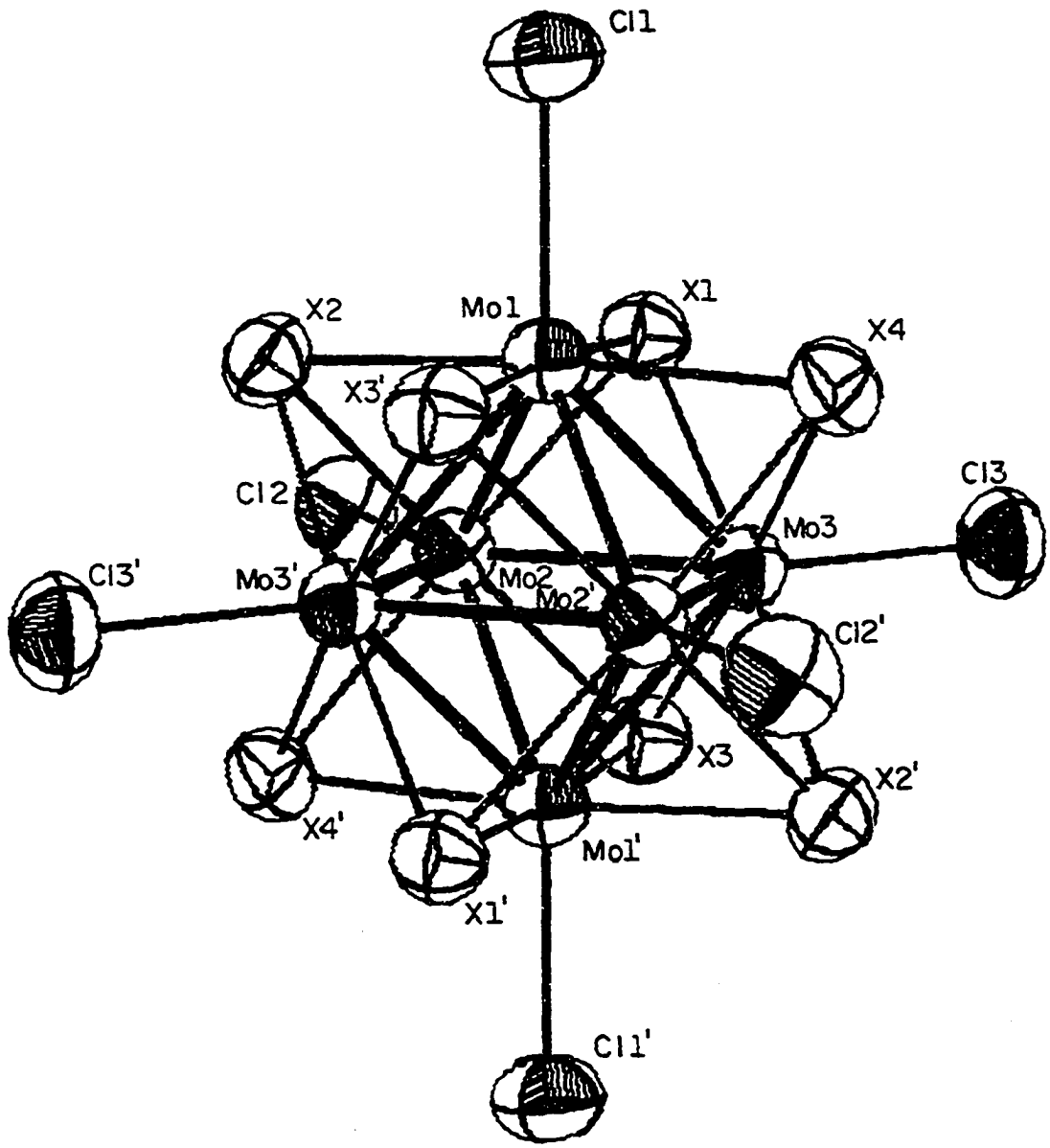

Figure 6. A labelled perspective view of the 50% probability thermal ellipsoids of the $(Mo_6Cl_7S)Cl_6^{3-}$ cluster

Table VIII. Bond distances (Å), nonbonded distances (Å), and angles (deg) in $(Mo_6Cl_7S)Cl_6^{3-}$ cluster of $(C_5H_5NH)_3[(Mo_6Cl_7S)Cl_6]\cdot 3(C_5H_5NH)Cl$[a]

Bond Distances			
Mo(1)-Mo(2)	2.608(2)	X(2)-Mo(1)	2.473(3)
Mo(1)-Mo(2')	2.612(2)	X(2)-Mo(2)	2.477(3)
Av Mo-Mo	2.610	X(2)-Mo(3')	2.474(3)
Cl(1)-Mo(1)	2.456(3)	Av X(2)-Mo	2.475
		X(1)-Mo(1)	2.473(5)
		Av X-Mo	2.475
Nonbonded Distances			
X(2)-X(1)	3.499(6)		
X(2)-X(3')	3.493(5)		
Av X-X	3.495		
Angles			
Mo(2)-Mo(1)-Mo(3)	60.00	Mo(1)-X(1)-Mo(2)	63.7(1)
Mo(2)-Mo(1) Mo(3')	60.05(3)	Mo(1)-X(2)-Mo(2)	63.59(9)
Mo(2')-Mo(1)-Mo(3)	60.05(3)	Mo(1)-X(2)-Mo(3')	63.74(9)
Mo(2')-Mo(1)-Mo(3')	59.89(5)	Mo(2)-X(2)-Mo(3')	63.69(8)
Av Mo-Mo-Mo	60.00	Av Mo-X-Mo	63.7
X(1)-Mo(1)-X(4)	90.0(1)	X(1)-Mo(1)-Cl(1)	91.5(1)
X(1)-Mo(1)-X(2)	90.1(1)	X(2)-Mo(1)-Cl(1)	91.8(1)
X(2)-Mo(1)-X(3')	89.83(8)	X(3')-Mo(1)-Cl(1)	93.0(1)
X(3')-Mo(1)-X(4)	89.75(9)	X(4)-Mo(1)-Cl(1)	92.7(1)
Av X-Mo-X	89.8	Av X-Mo-Cl	92.3

[a] X(1), X(1') occupy crystallographic special positions on the cluster's 3-fold axis; the other 6 bridging ligands are all equivalent, as are all 6 Mo, and all 6 Cl.

Table IX. Bond distances (Å) and nonbonded distances (Å) in $(Mo_6Cl_7S)Cl_6^{3-}$ clusters of $(C_5H_5NH)_3[(Mo_6Cl_7S)Cl_6]$

	c sites	b sites
	Bond Distances	
Mo(1)-Mo(2)	2.599(2)	2.601(2)
Mo(1)-Mo(3)	2.597(1)	2.607(2)
Mo(1)-Mo(2')	2.617(2)	2.594(2)
Mo(1)-Mo(3')	2.611(2)	2.600(2)
Mo(2)-Mo(3)	2.600(1)	2.596(2)
Mo(2)-Mo(3')	2.609(2)	2.610(2)
Av Mo-Mo	2.606	2.601
Mo(1)-Mo(1')	3.688(2)	3.674(2)
Mo(2)-Mo(2')	3.688(3)	3.672(2)
Mo(3)-Mo(3')	3.678(2)	3.690(2)
X(1)-Mo(1)	2.451(4)	2.484(4)
X(1)-Mo(2)	2.464(4)	2.473(4)
X(1)-Mo(3)	2.458(4)	2.467(4)
Av X(1)-Mo	2.458	2.475
X(2)-Mo(1)	2.473(4)	2.471(4)
X(2)-Mo(2)	2.477(4)	2.478(4)
X(2)-Mo(3')	2.483(4)	2.470(4)
Av X(2)-Mo	2.478	2.473
X(3)-Mo(1')	2.492(4)	2.456(4)
X(3)-Mo(2)	2.468(4)	2.462(4)
X(3)-Mo(3)	2.487(4)	2.458(4)
Av X(3)-Mo	2.482	2.459
X(4)-Mo(1)	2.478(3)	2.482(4)
X(4)-Mo(2')	2.486(4)	2.467(4)
X(4)-Mo(3)	2.476(4)	2.492(4)
Av X(4)-Mo	2.480	2.480

Table IX. (continued)

	c sites	b sites
	Bond Distances	
Av X-Mo	2.474	2.472
Mo(1)-Cl(1)	2.449(4)	2.461(4)
Mo(2)-Cl(2)	2.451(4)	2.450(4)
Mo(3)-Cl(3)	2.451(3)	2.459(4)
	Nonbonded Distances	
X(1)-X(2)	3.491(6)	3.506(5)
X(1)-X(3)	3.492(5)	3.487(5)
X(1)-X(4)	3.482(5)	3.515(5)
X(2)-X(3')	3.516(5)	3.478(5)
X(2)-X(4')	3.507(5)	3.490(5)
X(3)-X(4')	3.493(5)	3.481(5)
Av X-X	3.497	3.493

Table X. Angles (deg) within the $(Mo_6Cl_7S)Cl_6^{3-}$ clusters of $(C_5H_5NH)_3[(Mo_6Cl_7S)Cl_6]$

	c sites	b sites
Mo(2)-Mo(1)-Mo(3)	60.03(4)	59.79(5)
Mo(2)-Mo(1)-Mo(3')	60.09(4)	60.25(5)
Mo(2')-Mo(1)-Mo(3)	60.04(5)	60.24(5)
Mo(2')-Mo(1)-Mo(3')	59.64(4)	59.97(5)
Mo(1)-Mo(2)-Mo(3)	59.95(4)	60.24(5)
Mo(1)-Mo(2)-Mo(3')	60.19(5)	59.86(4)
Mo(1')-Mo(2)-Mo(3)	60.08(4)	60.13(4)
Mo(1')-Mo(2)-Mo(3')	59.61(4)	60.14(5)
Mo(1)-Mo(3)-Mo(2)	60.02(4)	59.98(5)
Mo(1)-Mo(3)-Mo(2')	60.35(4)	59.62(5)
Mo(1')-Mo(3)-Mo(2)	60.29(3)	59.90(4)
Mo(1')-Mo(3)-Mo(2')	59.73(5)	59.90(5)
Av Mo-Mo-Mo	60.00	60.00
Mo(1)-X(1)-Mo(2)	63.85(10)	63.30(9)
Mo(1)-X(1)-Mo(3)	63.88(10)	63.57(9)
Mo(2)-X(1)-Mo(3)	63.76(10)	63.40(9)
Mo(1)-X(2)-Mo(2)	63.35(9)	63.42(9)
Mo(1)-X(2)-Mo(3')	63.60(9)	63.50(9)
Mo(2)-X(2)-Mo(3')	63.47(10)	63.68(9)
Mo(1')-X(3)-Mo(2)	63.68(9)	63.66(9)
Mo(1')-X(3)-Mo(3)	63.26(10)	63.89(10)
Mo(2)-X(3)-Mo(3)	63.29(8)	63.68(10)
Mo(1)-X(4)-Mo(2')	63.63(9)	63.21(9)
Mo(1)-X(4)-Mo(3)	63.24(8)	63.23(9)
Mo(2')-X(4)-Mo(3)	63.43(9)	63.51(9)
Av Mo-X-Mo	63.54	63.50
X(1)-Mo(1)-X(2)	90.3(1)	90.1(1)
X(1)-Mo(1)-X(4)	89.9(1)	90.1(1)

Table X. (continued)

	c sites	b sites
X(2)-Mo(1)-X(3')	90.2(1)	89.8(1)
X(3')-Mo(1)-X(4)	89.3(1)	89.7(1)
X(1)-Mo(2)-X(2)	89.9(1)	90.2(1)
X(1)-Mo(2)-X(3)	90.2(1)	89.9(1)
X(2)-Mo(2)-X(4')	89.9(1)	89.8(1)
X(3)-Mo(2)-X(4')	89.7(1)	89.9(1)
X(1)-Mo(3)-X(3)	89.9(1)	90.1(1)
X(1)-Mo(3)-X(4)	89.8(1)	90.3(1)
X(2')-Mo(3)-X(3)	90.0(1)	89.8(1)
X(2')-Mo(3)-X(4)	90.0(1)	89.4(1)
Av X-Mo-X	89.9	89.9
X(1)-Mo(1)-Cl(1)	91.6(2)	90.0(1)
X(2)-Mo(1)-Cl(1)	91.7(1)	91.1(1)
X(3')-Mo(1)-Cl(1)	92.9(1)	94.4(2)
X(4)-Mo(1)-Cl(1)	92.5(1)	93.2(1)
X(1)-Mo(2)-Cl(2)	91.3(1)	91.2(1)
X(2)-Mo(2)-Cl(2)	93.1(1)	91.6(1)
X(3)-Mo(2)-Cl(2)	90.9(1)	92.9(1)
X(4')-Mo(2)-Cl(2)	93.5(1)	92.5(1)
X(1)-Mo(3)-Cl(3)	92.4(1)	90.7(1)
X(2')-Mo(3)-Cl(3)	91.9(1)	93.6(1)
X(3)-Mo(3)-Cl(3)	92.3(1)	92.3(2)
X(4)-Mo(3)-Cl(3)	91.9(1)	92.6(1)
Av X-Mo-Cl	92.2	92.2

Table XI. Bond distances (Å) in the pyridinium cations of both compounds

Cation No. 1[a]		Cation No. 2[a]	
N(1)-C(1)	1.34(3)	N(2)-C(6)	1.57(3)
C(1)-C(2)	1.44(3)	C(6)-C(7)	1.44(3)
C(2)-C(3)	1.44(4)	C(7)-C(8)	1.33(3)
C(3)-C(4)	1.46(4)	C(8)-C(9)	1.33(3)
C(4)-C(5)	1.24(3)	C(9)-C(10)	1.27(3)
C(5)-N(1)	1.38(3)	C(10)-N(2)	1.35(3)
Av C-C	1.37		1.34
Av C-N	1.36		1.46
Cation No. 3[a]		Cation[b]	
N(3)-C(11)	1.43(3)	R(1)-R(2)	1.27(3)
C(11)-C(12)	1.39(3)	R(2)-R(3)	1.37(3)
C(12)-C(13)	1.32(3)	R(3)-R(4)	1.33(3)
C(13)-C(14)	1.36(3)	R(4)-R(5)	1.32(3)
C(14)-C(15)	1.37(3)	R(5)-R(6)	1.39(3)
C(15)-N(3)	1.31(3)	R(6)-R(1)	1.27(3)
Av C-C	1.36	Av R-R	1.33
Av C-N	1.37		

[a]Pyridinium cations of $(C_5H_5NH)_3[(Mo_6Cl_7S)Cl_6]$.

[b]Pyridinium cation of $(C_5H_5NH)_3[(Mo_6Cl_7S)Cl_6]\cdot 3(C_5H_5NH)Cl$.

Table XII. Average bond distances (Å) in selected Mo_6X_8 cluster compounds

	Mo-Mo	$Mo-X_b$	Reference
$(Mo_6Cl_8)Cl_{4/2}Cl_2$	2.607(2)	2.471(2)	20
$Hg[(Mo_6Cl_8)Cl_6]$	2.62(1)	2.48(2)	72
$(Mo_6Cl_7Se)Cl_{6/2}$	2.616(1)	2.495(1)	73
$(C_5H_5NH)_3[(Mo_6Cl_7S)Cl_6]$	2.606(2)	2.474(4)	this work
	2.601(2)	2.472(4)	
$(C_5H_5NH)_3[(Mo_6Cl_7S)Cl_6]\cdot 3(C_5H_5NH)Cl$	2.610(2)	2.475(5)	this work
Mo_6S_8	2.780	2.439	10
$PbMo_6S_8$	2.705(3)	2.455(9)	9

Inspection of Tables VIII and IX reveals that there are small, but statistically significant variations among corresponding distances within the 3 $(Mo_6Cl_7S)Cl_6^{3-}$ clusters. The maximum difference among the Mo-Mo distances is only 0.023Å. As shown in Table XII, the average Mo-Mo bond lengths for the 3 clusters fall in a narrow range, and are in good agreement with the values observed for the isolectonic $Mo_6Cl_8^{4+}$ clusters of Mo_6Cl_{12} and $Hg[(Mo_6Cl_8)Cl_6]$ and the isoelectronic $Mo_6Cl_7Se^{3+}$ cluster of $Mo_6Cl_{10}Se$.

The average Mo-X_b bond lengths of the three $Mo_6Cl_7S^{3+}$ clusters fall between 2.472 and 2.475Å, in excellent agreement with the Mo-Cl_b bond lengths of the isoelectronic $Mo_6Cl_8^{4+}$ cluster compounds. By analogy to the $Mo_6Cl_7Se^{3+}$ cluster, the sulfide is most likely statistically disordered over the 8 bridging ligand sites of the $Mo_6Cl_7S^{3+}$ cluster.[73] Nevertheless, in case the sulfide were localized, the average Mo-X_b bond lengths of each of the independent bridging ligand sites were compared because the Mo-S_b bond is 0.02-0.04Å shorter than the Mo-Cl_b bond. The average Mo-X_b bond lengths of the X3b and X1c bridging ligands of $(pyH)_3[(Mo_6Cl_7S)Cl_6]$ are noticeably shorter than the values for the other bridging

ligands. In the $Mo_6Cl_7Se^{3+}$ cluster, the maximum variation among the average Mo-X_b bond lengths is only 0.010Å.[73] This may indicate sulfide is disordered over only 2 of the 8 bridging ligand sites of the $(Mo_6Cl_7S)^{3+}$ clusters of $(pyH)_3[(Mo_6Cl_7S)Cl_6]$.

The Mo-Cl_t bond lengths of the three $(Mo_6Cl_7S)Cl_6^{3-}$ clusters are equivalent, and, as shown in Table XIII, are anomalously long when compared to the Mo-Cl_t bond of Mo_6Cl_{12}. Interestingly, the Mo-Cl_t bond length of $(Mo_6Cl_7S)Cl_6^{3-}$ is nearly equal to the weighted average of the two Mo-Cl_t and the four Mo-Cl_{tt} bond lengths of Mo_6Cl_{12}. Furthermore, Table XIII indicates that the apparent bond order of the Mo-Cl_t bond of $(Mo_6Cl_7S)Cl_6^{3-}$ is commensurate with the average Mo-L_t bond orders of other $Mo_6X_8L_6$ clusters. Thus, the apparent strength of the bonding interaction between the molybdenum atoms and the terminal ligands is a constant for all these $Mo_6X_8L_6$ clusters. Considered in this light, the Mo-Cl_t bond length of the $(Mo_6Cl_7S)Cl_6^{3-}$ cluster is reasonable.

Table XIII. Average Mo-L bond lengths (Å) and bond orders in selected $(Mo_6X_8)L_6$ cluster compounds

Compound	L	Mo-L_t	Mo-L_{tt}	Est. Mo-L[a]	Av. Bond Order[b]
$(C_5H_5NH)_3[(Mo_6Cl_7S)Cl_6]$	Cl	2.454(4)	—	2.286	0.52
$(C_5H_5NH)_3[(Mo_6Cl_7S)Cl_6]\cdot 3(C_5H_5NH)Cl$	Cl	2.456(3)	—	2.286	0.52
$(Mo_6Cl_8)Cl_2Cl_{4/2}$[20]	Cl	2.379(1)	2.494(1)	2.286	0.53
$(Mo_6Br_8)Br_4(H_2O)_2$[23]	Br	2.587(2)	—	2.436	0.51
	H_2O	2.191(18)	—	1.956	
$Cs_2[(Mo_6Cl_8)Br_6]$[74]	Br	2.59(1)	—	2.436	0.55
$(Mo_6Cl_7Se)Cl_{6/2}$[73]	Cl	—	2.514(1)	2.286	0.42

[a]Estimated by adding Pauling covalent radius of nonmetal[25] to Pauling metallic radius for molybdenum.[21]

[b]Calculated from Pauling's formula: bond order = $10^{[(\text{Est Mo-L})-(\text{Mo-L})]/.6}$.

PART II. SYNTHESIS AND STRUCTURE OF $(Mo_6S_{\sim 6}Cl_{\sim 2})(NC_5H_5)_6$, A MOLECULAR CLUSTER RELATED TO THE CHEVREL PHASES

INTRODUCTION

Since the initial report by Chevrel and coworkers[1] of a new class of binary and ternary molybdenum chalcides Mo_6Y_8 and $M_nMo_6Y_8$ (M = metal cation; Y=S, Se, Te; n=0 to 4), the preparations,[2-6] structures,[7-12] and physical properties[13-17] of a large number of derivatives have been reported. This extensive activity was spurred on by the discovery that many of these "Chevrel phases" are superconductors.[18] Several derivatives have moderately high critical temperatures (10-15°K) and extremely high critical fields (400-600 kG).

The structure of the Chevrel phases can be visualized as a trigonally distorted simple cubic lattice of chalcide ions, with every eighth cube occupied by a metal-metal bonded octahedral cluster of molybdenum atoms. The occupied cube defines a Mo_6Y_8 cluster unit, illustrated in Figure 7. The eight chalcides are termed "bridging ligands", since each is bound to a triangular face of the octahedron. In addition to bonding to four other molybdenum atoms and to four bridging ligands (a face of the cube), each molybdenum atom has a coordination site on the normal to the cube face. This "terminal ligand" site is filled by a bridging ligand of a neighboring cluster, as shown in Figure 7.

The strong bonding between a cluster and each of its six neighboring clusters broadens the metal-metal bonding molecular orbitals of individual clusters into narrow bands.[28,31]

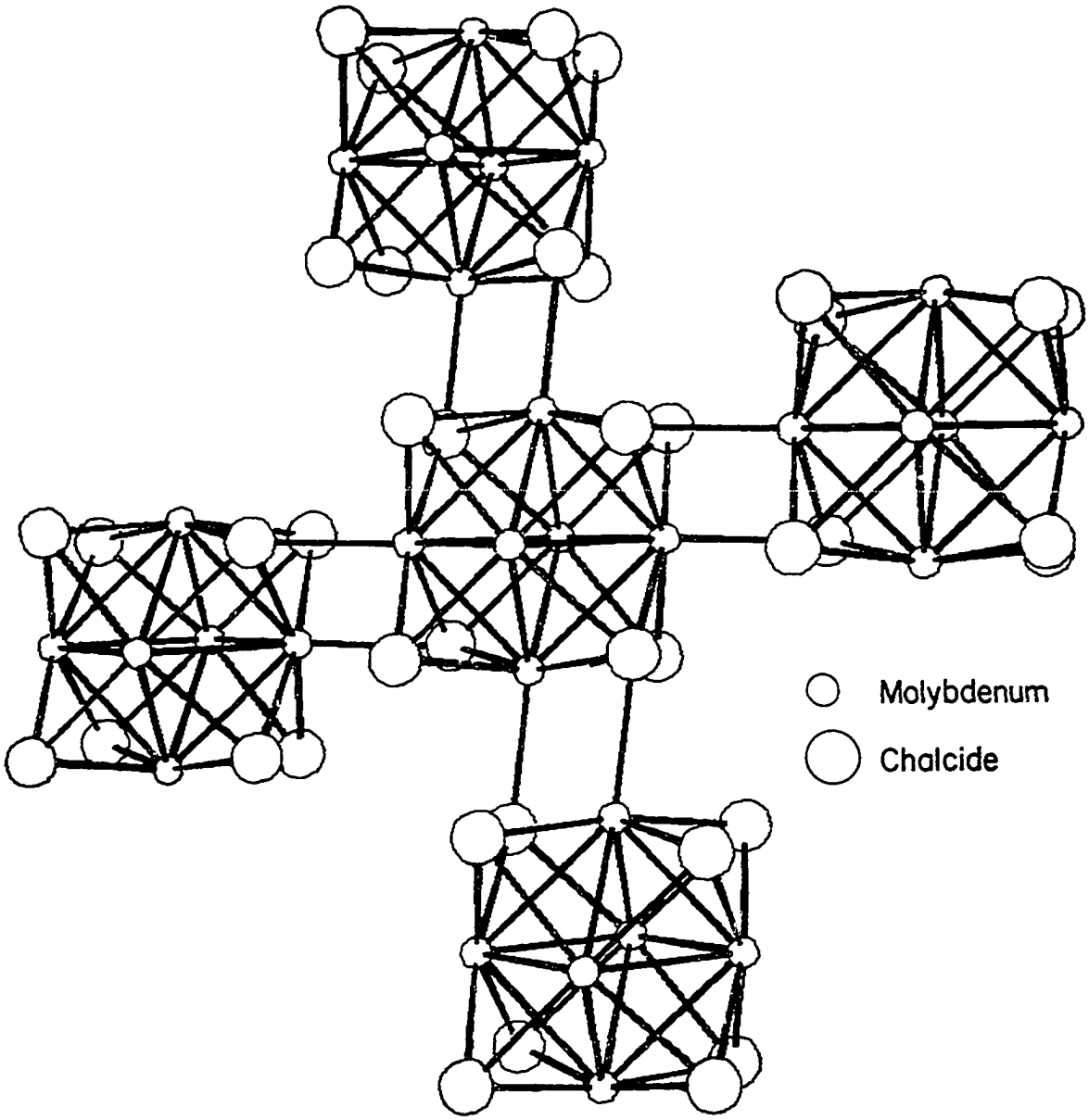

Figure 7. A perspective view of the arrangement of Mo_6X_8 clusters in the Chevrel phases, with two of the six neighboring clusters deleted

The conduction band in these compounds consists of one or more of these "metal-metal bonding" bands. A variety of metal atoms has been inserted into open channels which exist in the structure of the Chevrel phases, forming ternary Chevrel phases. The ternary metal atom's valence electrons are donated to the conduction band, thus increasing the number of electrons available for Mo-Mo bonding in the Mo_6Y_8 cluster from twenty in the binary Chevrel phases to a value between twenty and twenty-four in the ternary compounds.

The Mo_6Y_8 cluster of the Chevrel phases is strikingly similar to the twenty-four electron $Mo_6X_8^{4+}$ cluster of the α-molybdenum(II) halides and their derivatives.[19,23] The important difference is that the terminal ligand sites of the $Mo_6X_8^{4+}$ cluster are filled by six terminal ligands, not by bridging ligands of neighboring clusters as in the Chevrel phases. These terminal ligands in the α-molybdenum(II) halide structure can be shared between clusters (as in α-molybdenum(II) chloride,[19] best formulated as $[(Mo_6Cl_8)Cl_{4/2}Cl_2]$), but they nonetheless block the close approach between neighboring clusters found in the Chevrel phase structure. Because there is no intercluster Mo-Mo interaction, the α-molybdenum(II) halides and their derivatives are not electrical conductors.

The Mo_6X_8 cluster unit is the building block for the structures of the α-molybdenum(II) halides and the Chevrel

phases. This cluster is a sufficiently stable building block that it can accommodate the two quite different patterns of assembly in the structures of these two classes of compounds. This observation prompted us to attempt the preparation of halide-chalcide clusters, $Mo_6X_{8-n}Y_n$ (n=1, ..., 7). In this paper we report the preparation and crystal and molecular structure of $(Mo_6S_{\sim 6}Cl_{\sim 2})(NC_5H_5)_6$, the first example of a molecular Mo_6X_8 cluster compound with fewer than 24 electrons involved in metal-metal bonding. Despite the determination of the molecular structure, the chloride and sulfide compositions are known only approximately because:

a) very limited analytical data are available for the compound;

b) the "compound" appears to form a molecular solid solution, with a range of chloride and sulfide compositions.

The formulation will be indicated as $(Mo_6S_6Cl_2)(NC_5H_5)_6$ throughout the remainder of this paper.

EXPERIMENTAL

Materials

Cert. ACS grade pyridine (Fischer Scientific Co.) was vacuum distilled onto outgassed 4A molecular sieves, and was vacuum distilled as needed. Cert. ACS grade methanol (Fischer Scientific Co.) was either used as received, or stored over outgassed 3A molecular sieves, and vacuum distilled as needed. Molybdenum(V) chloride (Research Organic/Inorganic Chemical Corp.) was stored in a dry box (dew point ca. -75°C) under a nitrogen atmosphere. Aluminum (99.99%) and hydrogen sulfide (Matheson Gas Prod.) were used as received. Sodium metal (Fischer Scientific Co.) was rinsed in cyclohexane and absolute ethanol, then placed into the reaction flask under a nitrogen atmosphere. Aluminum(III) chloride (Fischer Scientific Co.) was sublimed at 150°C under dynamic vacuum prior to use. α-Molybdenum(II) chloride was prepared according to the method of Dorman and McCarley.[48] In this procedure, molybdenum(V) chloride is reduced by aluminum in an aluminum chloride-rich sodium tetrachloroaluminate melt. The molybdenum(II) chloride product is extracted into an ethanol solution. Addition of hydrochloric acid and evaporation of the solution produces crystals of $(H_3O)_2[(Mo_6Cl_8)Cl_6]\cdot 6H_2O$. Heating this product at 350°C in vacuo for 24 hours yields pure, anhydrous $(Mo_6Cl_8)Cl_4$.

Anhydrous sodium hydrosulfide was prepared by reaction of hydrogen sulfide with sodium ethoxide, using the procedure described by Brauer.[49]

Syntheses

Preparation of $(Mo_6S_6Cl_2)(NC_5H_5)_6$

0.5g Mo_6Cl_{12} (0.5 mmole) and 0.22g NaSH (3.9 mmole) were weighed into a 13 mm OD pyrex tube of ca. 20 cm length in the dry box. After closing the valve attached to the tube, the tube was transferred to a vacuum line (working vacuum of 10^{-4} - 10^{-5} torr) and outgassed. Ca. 9 mL of dry pyridine were vacuum distilled onto the solid mixture in the tube. When the distillation had been completed, the contents of the tube were warmed to ca. 35°C. Vigorous bubbling occurred, and the slurry changed from a pale yellow to a red-orange color. The bubbling ceased after about ten minutes. The slurry was refrozen and outgassed, and the tube was then sealed off with a torch. The reaction tube was heated in an upright position for three days at 200 ±5°C (caution--the vapor pressure of pyridine at this temperature is approximately 8 atmospheres; explosions may occur if the tube is not properly sealed off). The tube was slowly cooled to room temperature over a period of a day. The product consisted of a plug of microcrystalline solids at the bottom of the tube, and a mixture of brown and red crystals deposited on top of

the plug, and on the sides of the tube. The crystals were separated from the plug by decantation, filtered from the pale brown pyridine solution and washed with methanol. The less abundant red crystals were manually separated from the desired bowwn crystals under a microscope. Because of this tedious separation, the best yield of pure crystals of $(Mo_6S_6Cl_2)(NC_5H_5)_6$ has been ca. 10 mg. Anal. Calcd.: S, 14.64. Found: S, 13.91.

Preparation of $(Mo_6S_5Cl_3)(NC_5H_5)_3$

1.00g Mo_6Cl_{12} (1.0 mmole) and 0.96g NaSH (16 mmole) were weighed into a 100 mL Schlenk reflux flask equipped with a water-cooled condenser in the dry box. The flask was transferred to the vacuum line and outgassed. Ca. 75 mL of dry pyridine were distilled into the flask. The reaction mixture was refluxed under a nitrogen atmosphere 12-14 hours. The insoluble brown product was extracted with dry methanol 1-2 days. Anal. Calcd. for $(Mo_6S_5Cl_3)(NC_5H_5)_3$: Mo, 53.32; S, 14.85; Cl, 9.85; N, 3.89; C, 16.69; H, 1.40. Found: Mo, 51.99; S, 15.67; Cl, 9.45; N, 3.60; C, 15.73; H, 1.55.

Preparation of $(Mo_6S_7Cl)(NC_5H_5)_5$

0.5g Mo_6Cl_{12} (0.5 mmole), 0.28g NasH (5 mmole) and 0.016g S (0.5 mmole) were weighed into a 13 mm OD pyrex tube in the dry box. The procedure was identical to that used

for the preparation of $(Mo_6S_6Cl_2)(NC_5H_5)_6$. The entire insoluble product (brown powder and brown crystals) was extracted with dry methanol for 1 day. Anal. Calcd. for $(Mo_6S_7Cl)(NC_5H_5)_5$: Mo, 46.76; Cl, 2.88; N, 5.69; C, 24.39; H, 2.05. Found: Mo, 45.39; Cl, 2.56; N, 5.62; C, 24.13; H, 2.07.

X-ray Structure Determination

Collection and reduction of x-ray data

$(Mo_6S_6Cl_2)(NC_5H_5)_6$ crystallizes as thin brown parallelipipeds. A single crystal with dimensions 0.5 x 0.02 x 0.06 mm was selected and mounted with its long axis nearly collinear with Φ on an automated four-circle diffractometer.[52] Ten different reflections were selected from ω-oscillation photographs taken at Φ=0°, 30°, 60°, 90°. The angular coordinates of the ten reflections were input to the automatic indexing program ALICE,[53] which calculated the orientation matrix, the reduced unit cell, and the reduced cell scalars. These approximate cell parameters and the scalars indicated triclinic crystal symmetry. X-ray data were collected using graphite monochromatized Mo Kα radiation within a sphere defined by $2\theta \leq 50°$ in the hkl, $\bar{h}\bar{k}l$, $h\bar{k}\bar{l}$, and $\bar{h}k\bar{l}$ octants. The intensities of three strong reflections, checked after every 75 reflections, remained approximately constant throughout data collection, indicating there was no

significant crystal or instrument instability. Intensity data were corrected for Lorentz polarization effects. An absorption correction was made (μ=22.3 cm^{-1}) using a Φ scan technique. The intensity of the $\bar{4}\bar{2}\bar{3}$ reflection at χ=85.14° was monitored as a function of Φ, at 10° intervals. These intensities were input to the absorption correction program ABSN.[75] Accurate unit cell parameters and their estimated standard deviations were determined by a least squares fit to the $\pm 2\theta$ values of sixteen independent high angle ($2\theta \geq 25°$) reflections. The cell parameters are a=10.781(3)Å, b=11.856(2)Å, c=9.408(1)Å, α=90.42(2)°, β=109.44(2)°, γ=65.49(2)°; with Z=1, ρ_{calc}=2.14 g cm^{-3}.

Solution and refinement of the structure

1,969 reflections with $I > 3\sigma_I$ were measured. Equivalent reflections (at least one of the three indices =0) were averaged; twenty with $|F_o - F_a|/|F_a| > 0.20$ were discarded. Thus 1,606 independent reflections were used in the structure refinement. Since a Howells, Phillips and Rodgers test indicated a centric space group, the structure was refined in the space group $P\bar{1}$. Using Patterson superposition techniques,[54] three independent molybdenum atom positions were located. The four independent bridging ligand positions were located in an electron density map phased by the molybdenum atoms.[55] The inversion operation generates the other half

of the single Mo_6X_8 cluster in the unit cell. (Note: Because of the very similar x-ray scattering power of chlorine and sulfur, we were unable to distinguish them among the 4 independent bridging ligand sites of the $(Mo_6S_6Cl_2)py_6$ (py=C_5H_5N) clusters. The scattering factor of sulfur was used in the refinement of the bridging ligand parameters). A discrepancy factor ($R=\Sigma||F_o|-|F_c||/\Sigma|F_o|$) of 0.180 resulted from refinement of the positional and isotropic thermal parameters of these seven independent atoms. The carbon and nitrogen atom positions were located in subsequent sharpened electron density maps.[56] All non-hydrogen atoms in the structure except those in pyridine ring 1 were refined anisotropically by full matrix least squares techniques, minimizing the function $\Sigma w(|F_o|-|F_c|)^2$, where $w=1/\sigma_F^2$.[56] Because of the large thermal parameters associated with several carbon atoms of ring 1, the atoms in this ring were refined isotropically. The scattering factors of Hanson et al.[57] were used, with molybdenum and sulfur corrected for the real and imaginary parts of anomalous dispersion.[58] The final discrepancy factors were R=0.084 and $R_w=[\Sigma w(|F_o|-|F_c|)^2/\Sigma w(F_o)^2]^{1/2}=0.099$. There was no significant electron density (>1e/$\mathring{A}^3$) in the final electron density difference map. Positional and thermal parameters are listed in Tables XIV and XV. Tables of observed and

of the single Mo_6X_8 cluster in the unit cell. (Note: Because of the very similar x-ray scattering power of chlorine and sulfur, we were unable to distinguish them among the 4 independent bridging ligand sites of the $(Mo_6S_6Cl_2)py_6$ (py=C_5H_5N) clusters. The scattering factor of sulfur was used in the refinement of the bridging ligand parameters). A discrepancy factor ($R=\Sigma||F_o|-|F_c||/\Sigma|F_o|$) of 0.180 resulted from refinement of the positional and isotropic thermal parameters of these seven independent atoms. The carbon and nitrogen atom positions were located in subsequent sharpened electron density maps.[56] All non-hydrogen atoms in the structure except those in pyridine ring 1 were refined anisotropically by full matrix least squares techniques, minimizing the function $\Sigma w(|F_o|-|F_c|)^2$, where $w=1/\sigma_F^2$.[56] Because of the large thermal parameters associated with several carbon atoms of ring 1, the atoms in this ring were refined isotropically. The scattering factors of Hanson et al.[57] were used, with molybdenum and sulfur corrected for the real and imaginary parts of anomalous dispersion.[58] The final discrepancy factors were R=0.084 and $R_w=[\Sigma w(|F_o|-|F_c|)^2/\Sigma w(F_o)^2]^{1/2}=0.099$. There was no significant electron density (>1e/$\mathring{A}^3$) in the final electron density difference map. Positional and thermal parameters are listed in Tables XIV and XV. Tables of observed and

calculated structure factor amplitudes are available as supplementary material.

Table XIV. Positional parameters for $(Mo_6S_6Cl_2)(NC_5H_5)_6$[a]

Mo(1)	0.4516(3)	0.3772(2)	0.5549(3)
Mo(2)	0.6243(3)	0.3849(2)	0.4155(3)
Mo(3)	0.6533(3)	0.4541(2)	0.6872(3)
X(1)	0.4274(8)	0.3206(6)	0.2967(8)
X(2)	0.4819(8)	0.4479(6)	0.8035(7)
X(3)	0.7164(7)	0.2346(6)	0.6470(7)
X(4)	0.1928(7)	0.5367(6)	0.4547(8)
N(1)	0.3967(26)	0.2232(21)	0.6288(25)
C(1)	0.2813(57)	0.2577(45)	0.6647(54)
C(2)	0.2368(59)	0.1646(52)	0.7109(57)
C(3)	0.3456(71)	0.0407(58)	0.7402(64)
C(4)	0.4543(82)	0.0059(66)	0.6815(82)
C(5)	0.4817(67)	0.1043(61)	0.6272(68)
N(2)	0.7716(25)	0.2451(18)	0.3064(22)
C(6)	0.7136(28)	0.2390(24)	0.1526(30)
C(7)	0.8031(33)	0.1559(33)	0.0820(34)
C(8)	0.9500(45)	0.0688(35)	0.1717(47)
C(9)	1.0002(40)	0.0770(31)	0.3285(39)
C(10)	0.9122(33)	0.1697(27)	0.3983(39)
N(3)	0.8436(25)	0.4006(22)	0.9152(24)
C(11)	0.8103(31)	0.4513(29)	1.0366(34)
C(12)	0.9260(43)	0.4178(35)	1.1797(40)
C(13)	1.0618(30)	0.3482(33)	1.1954(36)
C(14)	1.0953(36)	0.2950(36)	1.0733(40)
C(15)	0.9792(32)	0.3223(30)	0.9306(30)

[a]Numbers in parentheses are the estimated standard deviations of the coordinates and refer to the last significant digit of the preceding number.

Table XV. Thermal parameters for $(Mo_6S_6Cl_2)(NC_5H_5)_6$[a]

Atom	β_{11}	β_{22}	β_{33}	β_{12}	β_{13}	β_{23}
Mo(1)	10.4(4)	6.2(2)	12.1(4)	-2.7(2)	5.6(3)	-1.1(2)
Mo(2)	10.7(4)	6.1(2)	9.7(4)	-2.1(2)	4.7(3)	-0.4(2)
Mo(3)	10.2(4)	6.4(2)	10.4(4)	-2.6(2)	4.7(3)	-0.2(2)
X(1)	10(1)	6.5(6)	12(1)	-2.9(7)	4.1(8)	-1.0(6)
X(2)	10.7(9)	6.8(6)	8.5(9)	-3.4(7)	3.8(8)	-0.9(6)
X(3)	9(1)	5.7(6)	10(1)	-2.3(6)	3.7(8)	-0.5(6)
X(4)	8.3(9)	7.4(6)	11(1)	-2.9(6)	4.0(8)	-0.7(6)
N(2)	16(4)	6(2)	10(3)	-5(2)	9(3)	-4(2)
C(6)	10(4)	8(3)	12(4)	-1(3)	5(3)	-3(3)
C(7)	12(5)	18(5)	15(5)	-6(4)	9(4)	-2(4)
C(8)	24(8)	15(5)	26(8)	-8(5)	9(7)	5(5)
C(9)	22(6)	11(4)	17(6)	-1(4)	8(5)	1(4)
C(10)	12(5)	8(3)	25(7)	-1(3)	7(5)	0(4)
N(3)	13(4)	12(3)	12(4)	-6(3)	7(3)	0(2)
C(11)	11(4)	15(4)	14(5)	-10(4)	2(4)	-2(3)
C(12)	22(7)	19(5)	21(6)	-11(5)	14(6)	0(4)
C(13)	6(4)	19(5)	17(5)	-4(3)	5(4)	0(4)
C(14)	13(5)	19(5)	18(6)	-7(4)	-3(5)	1(4)
C(15)	11(4)	16(4)	11(4)	-5(3)	7(4)	-3(3)
N(1)[b]	4.4(5)					
C(1)	10(1)					
C(2)	11(1)					
C(3)	13(2)					
C(4)	16(2)					
C(5)	13(2)					

[a]The form of the anisotropic temperature factor expression is $\exp[-(\beta_{11}h^2+\beta_{22}k^2+\beta_{33}\ell^2+2\beta_{12}hk+2\beta_{13}h\ell+2\beta_{23}k\ell)]$. Values of β_{ij} are $x10^3$.

[b]The form of the isotropic temperature factor expression is $\exp[-\beta(\sin^2\theta/\lambda^2)]$.

RESULTS AND DISCUSSION

Synthesis of $(Mo_6S_6Cl_2)(NC_5H_5)_6$

One approach to the preparation of a mixed-ligand cluster $Mo_6X_{8-n}Y_n$ is to employ the same reaction conditions used in the synthesis of the binary cluster, but adding the second ligand to the reaction mixture. Chevrel and coworkers have demonstrated the feasibility of this approach for preparing molybdenum halide-chalcide clusters. Reaction of appropriate amounts of molybdenum, chalcogen, and either molybdenum(II) or molybdenum(III) halides at 1000°C for 24 hours yielded the new compounds $(Mo_6X_7Y)X_{6/2}$ (X=Cl, Br, I; Y=S, Se, Te).[73,76] Since these compounds are more closely related in structure and composition to the α-molybdenum(II) halides than to the Chevrel phases, it is not surprising that they are insulators.

Quite different results were achieved when the proportion of sulfur in the reaction mixture was increased. The two new compounds which resulted, $Mo_6S_6X_2$ (X=Br, I), are isomorphous with the Chevrel phases.[34] Significantly, these two compounds have rather high superconducting transition temperatures (13.8 and 14.0°K respectively).

A requisite for the success of this approach is thermodynamic stability of the desired product at 1000°C. Although most of the Chevrel phases meet this criterion, Mo_6S_8 is a notable exception,[10] decomposing at 468°C. It is certainly

conceivable that some members of the series $Mo_6X_{8-n}Y_n$ (n=1,2...,7) may also be thermodynamically unstable at high temperature, thus limiting the scope of this approach.

We chose to investigate the substitution of sulfide into the bridging ligand sites of the $Mo_6Cl_8^{4+}$ cluster as a route to $Mo_6Cl_{8-n}S_n$. $Mo_6Cl_8^{4+}$ was a logical choice as reactant because it undergoes bridging ligand substitution at moderate temperatures. Thus, substitution by bromide or iodide proceeds smoothly, yielding the stable $Mo_6Cl_4Y_4^{4+}$ or $Mo_6Y_8^{4+}$ clusters.[43,44] Studies of substitution by non-halides have been hampered by instability of the substituted products toward degradative oxidation. The only successes have been achieved with hydroxide and methoxide. Only two hydroxides can be substituted into the bridging ligand sites of $Mo_6Cl_8^{4+}$ before cluster decomposition occurs.[43,46] The cluster is slightly more tolerant toward substitution by methoxide. Complete substitution is possible, but the $Na_2[(Mo_6(OCH_3)_8)(OCH_3)_6]$ product is pyrophoric.[47]

The preparation of the $Mo_6Cl_7S^{3+}$ cluster[77] and the $Mo_6S_6Cl_2$ cluster establishes that stable chloride-sulfide clusters can be prepared by substitution of sulfide into the $Mo_6Cl_8^{4+}$ cluster. The reaction leading to $(Mo_6S_6Cl_2)py_6$ commences with vigorous bubbling, caused by dissolution of the amorphous, highly reactive Mo_6Cl_{12} in pyridine. The subsequent change in color of the solution from pale yellow

to red-orange signals substitution by hydrosulfide into the more reactive terminal ligand sites of the cluster. This assertion can be verified by reacting the red-orange solid, which precipitates if the reaction mixture is left at room temperature for several hours, with hydrochloric acid:

$$(2+x)\ HCl + "(Mo_6Cl_8)(SH)_xCl_{4-x}py_2" \longrightarrow$$

$$(pyH)_2[(Mo_6Cl_8)Cl_6] + x\ H_2S.$$

The sulfides in terminal ligand sites are replaced by chloride. However, similar treatment of the $Mo_6Cl_7S^{3+}$ cluster does not displace the bridging sulfide.[77] During subsequent prolonged heating of the reaction mixture at 200°C, sulfide substitutes into the cluster's bridging ligand sites. However, even under these conditions the substitution does not proceed cleanly. The contamination of the brown parallelipiped crystals with red crystals (presumably a less extensively substituted cluster product) is most likely caused by poor mixing of reactants in the sealed tube. Because of similar solubility properties of the red crystals and the parallelipipeds, a chemical separation of the two compounds has not been achieved. The bulk product of the reaction (brown powder) is similarly contaminated. Thus, only limited analytical data have been obtained on very small

quantities of parallelipiped crystals isolated by Pasteur's method.

There is little doubt that the bridging sulfides of $(Mo_6S_6Cl_2)py_6$ are deprotonated. A triply-bridging SH^- ligand is unknown, presumably because it is quite acidic. The stage of the reaction during which deprotonation occurs is not known. A significant amount of hydrogen gas was detected in the vapor above the reaction mixture (mass spectrum), indicating that the protons have oxidized the Mo_6X_8 cluster. In the starting material, the $Mo_6Cl_8^{4+}$ cluster has 24 electrons in the metal-metal bonding orbitals; in the product, the $Mo_6S_6Cl_2$ cluster has ca. 22 electrons. Based on bonding schemes for the Chevrel phases and the α-Mo(II) halides, the two electrons have been removed from a filled E_g metal-metal bonding orbital.[23,31] Magnetic measurements confirm that $(Mo_6S_6Cl_2)py_6$ is paramagnetic; the magnetic behavior is complicated, and will be the subject of further study. Although the number of electrons involved in metal-metal bonding can vary from 20-24 in the Mo_6S_8 cluster of the Chevrel phases, a $Mo_6X_8L_6$ cluster (α-Mo(II) halide or derivative) with fewer than 24 metal-metal bonding electrons is without precedent. The only examples of "electron-deficient" $M_6X_8L_6$ clusters are: $(W_6Br_8)Br_6$,[78] $(W_6Br_8)Br_4(Br_4)_{2/2}$,[78,79] $(W_6Br_8)Br_2(Br_4)_{4/2}$,[78]

all with 22 electrons; $(Nb_6I_8)I_{6/2}$,[80,81] with 19 electrons; and $Cs[(Nb_6I_8)I_{6/2}]$,[82] with 20 electrons.

Description of the Structure

Two different views of the molecular structure of $(Mo_6S_6Cl_2)py_6$ are provided in Figures 8 and 9.[69] The structure consists of an octahedral cluster of molybdenum atoms, with a bridging ligand bound to each face of the octahedron, and a pyridine nitrogen in each of the six terminal ligand sites. The important interatomic distances and angles are listed in Table XVI.[71] A cursory inspection of the Mo-Mo and Mo-X bond lengths and the Mo-Mo-Mo and Mo-X-Mo bond angles reveals that the Mo_6X_8 cluster has pseudo octahedral symmetry. When the pyridine rings in the terminal ligand sites are also considered, the highest possible molecular symmetry is D_{2h}. However, because the plane of each pyridine ring is not perpendicular to the nearest face of the X_8 cube, the molecular symmetry is reduced to C_i. In order to minimize contacts between pyridine and the bridging ligands, each pyridine ring should be coplanar with the plane of four of the molybdenum atoms. The actual angles are: between ring 1 and the (Mo1, Mo2, Mo1', Mo2') plane, 18.0°; between rings 2 and 3 and the (Mo2, Mo3, Mo2', Mo3') plane, 4.5 and 7.5° respectively. There are no pyridine-X contacts shorter than 3.40Å, which is ca. 0.05Å longer than the sum of the van der Waals radii.[22]

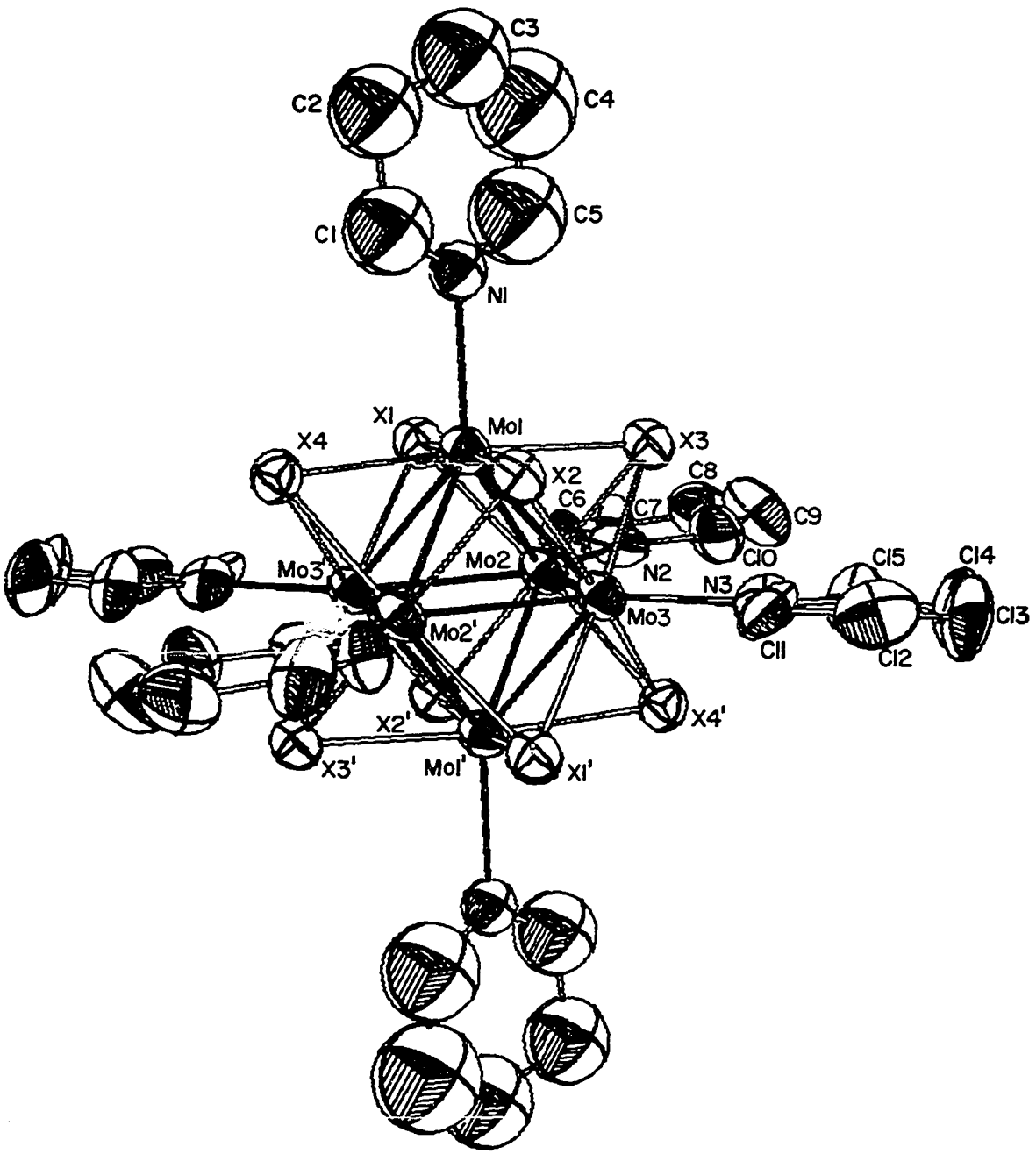

Figure 8. A labelled perspective view of the 50% probability thermal ellipsoids of the $(Mo_6S_6Cl_2)(NC_5H_5)_6$ cluster

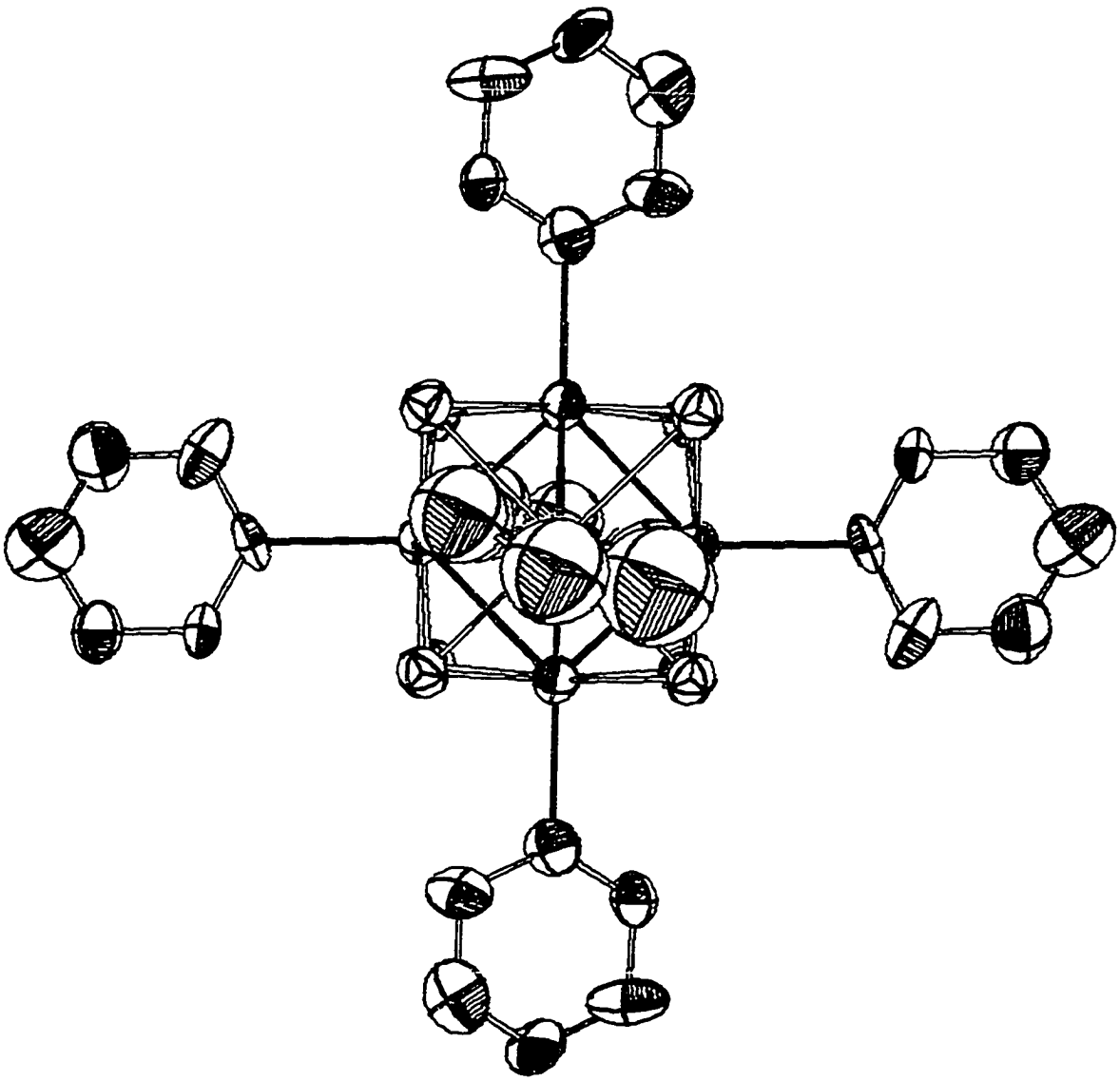

Figure 9. A perspective view down a pseudo 2-fold axis of the $(Mo_6S_6Cl_2)(NC_5H_5)_6$ cluster showing the 50% probability thermal ellipsoids

Table XVI. Interatomic distances (Å) and angles (deg) in $(Mo_6S_6Cl_2)(NC_5H_5)_6$

	Bond Distances		
Mo(1)-Mo(2)	2.639(3)	Ring No. 1	
Mo(1)-Mo(2')	2.633(3)	N(1)-C(1)	1.30(5)
Mo(1)-Mo(3)	2.634(4)	N(1)-C(5)	1.33(6)
Mo(1)-Mo(3')	2.635(3)	Av N(1)-C	1.32
Mo(2)-Mo(3)	2.638(3)	C(1)-C(2)	1.49(6)
Mo(2)-Mo(3')	2.626(3)	C(2)-C(3)	1.40(6)
Av Mo-Mo	2.634	C(3)-C(4)	1.37(8)
Mo(1)-Mo(1')	3.732(5)	C(4)-C(5)	1.45(8)
Mo(2)-Mo(2')	3.724(4)	Av C-C	1.43
Mo(3)-Mo(3')	3.721(5)		
X(1)-Mo(1)	2.474(7)	Ring No. 2	
X(1)-Mo(2)	2.467(8)	N(2)-C(6)	1.39(3)
X(1)-Mo(3')	2.464(7)	N(2)-C(10)	1.36(3)
Av X(1)-Mo	2.468	Av N(2)-C	1.38
X(2)-Mo(1)	2.444(7)	C(6)-C(7)	1.40(3)
X(2)-Mo(2')	2.469(7)	C(7)-C(8)	1.43(5)
X(2)-Mo(3)	2.465(7)	C(8)-C(9)	1.41(5)
Av X(2)-Mo	2.459	C(9)-C(10)	1.44(4)
X(3)-Mo(1)	2.476(7)	Av C-C	1.42
X(3)-Mo(2)	2.460(7)		
X(3)-Mo(3)	2.464(7)	Ring No. 3	
Av X(3)-Mo	2.467	N(3)-C(11)	1.37(3)
X(4)-Mo(1)	2.479(7)	N(3)-C(15)	1.33(3)
X(4)-Mo(2')	2.479(7)	Av N(3)-C	1.35
X(4)-Mo(3')	2.485(7)	C(11)-C(12)	1.42(4)
Av X(4)-Mo	2.481	C(12)-C(13)	1.30(4)
Av X-Mo	2.469	C(13)-C(14)	1.39(4)
N(1)-Mo(1)	2.31(2)	C(14)-C(15)	1.42(4)
N(2)-Mo(2)	2.28(2)	Av C-C	1.38
N(3)-Mo(3)	2.29(2)		
Av N-Mo	2.29		

Table XVI. (continued)

Nonbonded Distances			
X(1)-X(2')	3.501(9)	X(2)-X(3)	3.475(9)
X(1)-X(3)	3.491(9)	X(2)-X(4)	3.480(9)
X(1)-X(4)	3.498(9)	X(3)-X(4')	3.478(9)
		Av X-X	3.487

Angles			
Mo(2)-Mo(1)-Mo(3)	60.03(9)	Mo(1)-X(1)-Mo(2)	64.6(2)
Mo(2)-Mo(1)-Mo(3')	59.72(9)	Mo(1)-X(1)-Mo(3')	64.5(2)
Mo(2')-Mo(1)-Mo(3)	59.81(9)	Mo(2)-X(1)-Mo(3')	64.4(2)
Mo(2')-Mo(1)-Mo(3')	60.09(8)	Mo(1)-X(2)-Mo(2')	64.8(2)
Mo(1)-Mo(2)-Mo(3)	59.89(9)	Mo(1)-X(2)-Mo(3)	64.9(2)
Mo(1)-Mo(2)-Mo(3')	60.07(9)	Mo(2')-X(2)-Mo(3)	64.3(2)
Mo(1')-Mo(2)-Mo(3)	60.00(10)	Mo(1)-X(3)-Mo(2)	64.6(2)
Mo(1')-Mo(2)-Mo(3')	60.12(9)	Mo(1)-X(3)-Mo(3)	64.5(2)
Mo(1)-Mo(3)-Mo(2)	60.07(9)	Mo(2)-X(3)-Mo(3)	64.8(2)
Mo(1)-Mo(3)-Mo(2')	60.07(10)	Mo(1)-X(4)-Mo(2')	64.1(2)
Mo(1')-Mo(3)-Mo(2)	59.90(8)	Mo(1)-X(4)-Mo(3')	64.1(2)
Mo(1')-Mo(3)-Mo(2')	60.20(9)	Mo(2')-X(4)-Mo(3')	64.2(2)
Av Mo-Mo-Mo	60.00	Av Mo-X-Mo	64.5
X(1)-Mo(1)-X(3)	89.7(2)	X(1)-Mo(1)-N(1)	94.0(6)
X(1)-Mo(1)-X(4)	89.9(3)	X(2)-Mo(1)-N(1)	91.4(6)
X(2)-Mo(1)-X(3)	89.9(2)	X(3)-Mo(1)-N(1)	92.2(6)
X(2)-Mo(1)-X(4)	90.0(2)	X(4)-Mo(1)-N(1)	93.7(6)
X(1)-Mo(2)-X(2')	90.4(2)	X(1)-Mo(2)-N(2)	91.6(6)
X(1)-Mo(2)-X(3)	90.2(2)	X(2')-Mo(2)-N(2)	92.1(5)
X(2')-Mo(2)-X(4')	89.4(2)	X(3)-Mo(2)-N(2)	93.7(5)
X(3)-Mo(2)-X(4')	89.5(2)	X(4')-Mo(2)-N(2)	93.6(6)
X(1')-Mo(3)-X(2)	90.5(2)	X(1')-Mo(3)-N(3)	91.8(6)
X(1')-Mo(3)-X(4')	90.0(2)	X(2)-Mo(3)-N(3)	94.0(5)
X(2)-Mo(3)-X(3)	89.7(2)	X(3)-Mo(3)-N(3)	93.5(6)
X(3)-Mo(3)-X(4')	89.3(2)	X(4')-Mo(3)-N(3)	91.5(5)
Av X-Mo-X	89.9	Av X-Mo-N	92.8

Several bond lengths in the pyridine rings fall noticeably outside the range of values (1.34-1.40Å) observed in compounds where it is similarly coordinated,[83,84] presumably due to excessive thermal motion. The large thermal parameters of the atoms in the pyridine rings (particularly ring 1) are consistent with this hypothesis. The average Mo-N bond length is 2.29(2)Å, much longer than the average metal-nitrogen bond in $MoCl_3(NC_5H_5)_3$ (2.19(2)Å)[83] or $W_2Cl_6(NC_5H_5)_4$ (2.21(2)Å).[84] In Table XVII, the observed Mo-L_t (L_t=unshared terminal ligand) bond lengths of selected Mo_6X_8 clusters are compared to estimated values. The Mo-N bond of $(Mo_6S_6Cl_2)py_6$ is also exceptionally long within this group. The apparent weakness of this Mo-N bond may be compared with the elongated M-L_t bonds normally found for ligands occupying <u>trans</u> positions to bonds of multiple bond character, <u>e.g.</u>, M=O, M≡N, M≡M. In this case the four Mo-Mo bonds to adjacent atoms in the octahedron may be considered as acting comparably to the Mo≡Mo quadruple bond in $Mo_2(O_2CCF_3)_4 \cdot 2C_5H_5N$, where the Mo-N distance has been elongated to 2.548(8)Å.[85]

The Mo-X bond lengths vary from 2.444(7) to 2.485(7)Å, with an average value of 2.469(7)Å. A comparison of the average Mo-X bond lengths of the four independent bridging ligands reveals that all four bridging ligand sites are equivalent, within experimental error. Thus, we are unable

Table XVII. Average intramolecular distances in selected Mo_6X_8 cluster compounds

	Mo-Mo Bonding Electrons	Mo-Mo (Å)	Mo-X_b (Å)[a]	Terminal Ligand	Mo-L_t (Å)[a]	Estimated Mo-L_t (Å)[a,b]	Ref.
$(Mo_6Cl_8)Cl_2Cl_{4/2}$	24.0	2.607(1)	2.471(2)	Cl	2.379(3)	2.39	20
$(Mo_6Br_8)Br_4(H_2O)_2$	24.0	2 633(2)	2.601(2)	H_2O	2.19(2)	2.06	23
				Br	2.587(2)	2.54	
$(Mo_6S_6Cl_2)(NC_5H_5)_6$	22.0	2.634(3)	2.469(7)	NC_5H_5	2.29(2)	2.10	This work
$Cu_{3.66}Mo_6S_8$[c]	23.7	2.670	2.476	--	--	--	28
$Pb_{0.92}Mo_6S_{7.5}$[c]	22.8	2.704(3)	2.455(5)	--	--	--	9
Mo_6S_8C[c]	20.0	2.780	2.439	--	--	--	10

[a]Abbreviations: X_b=bridging ligand, L_t=unshared terminal ligand.

[b]Estimated by addition of covalent radius of ligand atom[25] to 1.40Å (estimated terminal bond radius of molybdenum).

[c]These compounds have no terminal ligands.

to discern any differences among the four bridging ligand sites from either the structure factors or the structural parameters, and can draw no conclusions about the arrangement of the sulfides and chlorides on the bridging ligand sites. As indicated in Table XVII, the average Mo-X_b bond length is nearly identical to the average Mo-Cl_b (Cl_b= bridging chloride) bond length in Mo_6Cl_{12}. The comparable Mo-S_b bond lengths in the Chevrel phases are slightly shorter, despite the higher average coordination number of these ligands. The disparity in bond lengths is made more striking by the fact that the covalent radius of sulfur is 0.05Å larger than that of chlorine.[24] Thus, the bond between molybdenum and the bridging ligand is apparently stronger in the Chevrel phases than in Mo_6Cl_{12} or $(Mo_6S_6Cl_2)py_6$.

The Mo-Mo bond lengths of selected Mo_6X_8 cluster compounds are listed in Table XVII for comparison with $(Mo_6S_6Cl_2)py_6$. Despite the fact that $Cu_{3.66}Mo_6S_8$ has ca. 1.7 more electrons in Mo-Mo bonding orbitals than $(Mo_6S_6Cl_2)py_6$, its Mo-Mo bond is 0.036Å longer. This is an indication that comparison with the Mo-Mo bonding in the Chevrel phases (e.g., $Cu_{3.66}Mo_6S_8$) is not valid, because intercluster Mo-Mo interaction undoubtedly detracts from intracluster Mo-Mo bonding in these compounds. On the

other hand, this complication does not muddle comparisons with the Mo-Mo bonding in the α-Mo(II) halides and their derivatives. The Mo-Mo bond in Mo_6Cl_{12}, which has 2 more electrons in Mo-Mo bonding orbitals, is 0.027Å shorter than the bond in $(Mo_6S_6Cl_2)py_6$. It is tempting to conclude that this slightly stronger bond is due to the 2 additional bonding electrons in Mo_6Cl_{12}. However, the Mo-Mo bond in $(Mo_6Br_8)Br_4(H_2O)_2$, which also has 24 electrons in Mo-Mo bonding orbitals, has the same length observed in $(Mo_6S_6Cl_2)py_6$. Presumably, the Mo-Mo bonding orbitals of $(Mo_6Br_8)Br_4(H_2O)_2$ mix more extensively with the ligand orbitals than is the case in Mo_6Cl_{12}, causing a slight destabilization, hence, lengthening, of the Mo-Mo bond. Thus, even comparison of the Mo-Mo bonding in $(Mo_6S_6Cl_2)py_6$ with that in the α-Mo(II) halides is somewhat tenuous. Furthermore, there are no structural data for oxidized or reduced versions of the α-Mo(II) halides for comparison.

By analogy to the Chevrel phases, it is reasonable to wonder whether the $(Mo_6X_8)py_6$ cluster might also accommodate a variable number of electrons (20-24) in its Mo-Mo bonding orbitals, yet remain isomorphous with $(Mo_6S_6Cl_2)py_6$. Thus, if the remainder of the series could be prepared, i.e., $(Mo_6S_4Cl_4)py_6$ (24 electrons), $(Mo_6S_5Cl_3)py_6$ (23 electrons), $(Mo_6S_7Cl)py_6$ (21 electrons), and $(Mo_6S_8)py_6$ (20 electrons), it might offer a unique opportunity to examine not only the

Mo-Mo bonding, but also the variation of spectroscopic and magnetic properties, solely as a function of the number of electrons in the Mo-Mo bonding orbitals.

There is evidence that part of this series may form a solid solution. A brown powder of approximate composition $(Mo_6S_5Cl_3)py_3$ was prepared by reaction of 16 equivalents of NaSH with Mo_6Cl_{12} in refluxing pyridine. The pyridine deficiency was presumably caused by the extensive extraction with methanol. The x-ray powder pattern (Debye-Scherrer camera) of $(Mo_6S_5Cl_3)py_3$ is nearly identical to that of $(Mo_6S_6Cl_2)py_6$. A very similar powder pattern is also observed for a brown powder with the composition $(Mo_6S_7Cl)py_5$, prepared by reacting Mo_6Cl_{12} with 10 equivalents of NaSH and 1 equivalent S at 200°C, followed by extraction with methanol. The similarity of all three powder patterns suggests that a solid solution $(Mo_6S_{5+x}Cl_{3-x})py_6$ $(0 \leq x \leq 2)$ exists. It is unlikely that a $(Mo_6S_6Cl_2)py_6$ impurity in the two powder samples is responsible for their powder patterns, because an electron spin resonance signal is observed for $(Mo_6S_6Cl_2)py_6$, but no signal is observed for $(Mo_6S_5Cl_3)py_3$. Further characterization of this series is planned.

The chemistry of $(Mo_6S_6Cl_2)py_6$ may also be interesting. It should be possible to replace the terminal pyridine ligands with other electron-pair donor ligands and promote solubility of the molecular unit in a variety of solvents.

At the same time it may be possible to eliminate the weakly bound terminal ligands and generate the ternary compound $Mo_6S_6Cl_2$, isomorphous with $Mo_6S_6Br_2$ and $Mo_6S_6I_2$.[34]

SUMMARY

Strong intracluster bonding endows the Mo_6X_8 cluster of the α-molybdenum(II) halides with impressive chemical stability. One manifestation of this stability is the preservation of the cluster's structural integrity during substitution reactions at the bridging ligand sites. For example, substitution by bromide or iodide into the $Mo_6Cl_8^{4+}$ cluster proceeds cleanly, yielding the $Mo_6X_8^{4+}$ (X=Br, I) clusters. However, previous attempts to substitute nonhalides into the $Mo_6Cl_8^{4+}$ cluster have led to cluster decomposition, or to substituted clusters of marginal stability. As described in this dissertation, stable sulfide-chloride Mo_6X_8 clusters have been prepared by substitution of sulfide into the $Mo_6Cl_8^{4+}$ cluster.

The $Mo_6Cl_7S^{3+}$ cluster was prepared by reaction of Mo_6Cl_{12} with two equivalents of NaSH in refluxing pyridine, and isolated as a pyridinium salt in the two compounds $(C_5H_5NH)_3[(Mo_6Cl_7S)Cl_6]$ and $(C_5H_5NH)_3[(Mo_6Cl_7S)Cl_6]\cdot 3(C_5H_5NH)Cl$. The structures of both compounds were determined by single crystal x-ray techniques. Corresponding bond distances and angles of the $(Mo_6Cl_7S)Cl_6^{3-}$ clusters in the two compounds are equivalent. The infrared spectra (200-450 cm^{-1}) of the two compounds are identical, and exhibit a band at 421 cm^{-1} assigned to a $(Mo_6Cl_7S)Cl_6^{3-}$

cluster vibration of predominant Mo-S character. Resolution of the chlorine 2p photoelectron spectra into components indicates not only that sulfide occupies a bridging ligand site in the $(Mo_6Cl_7S)Cl_6^{3-}$ cluster, but also that the difference in binding energy between the cluster's bridging and terminal chlorides is anomalously small.

The feasibility of stepwise substitution using this preparative procedure was investigated by reacting Mo_6Cl_{12} with six equivalents of NaSH. A disubstituted cluster was isolated as a pyridinium salt. Anal. Calcd. for $(H_3O)(C_5H_5NH)_3Mo_6Cl_{12}S_2 \cdot 5H_2O$: Mo, 40.69, Cl, 30.07; S, 4.53; C, 12.74; H, 2.21; N, 2.97. Found: Mo, 40.87; Cl, 29.44; S, 4.53; C, 12.88; H, 1.43; N, 2.94. These red crystals have a different morphology from either of the two previous compounds, and give a unique x-ray powder pattern. A good computer fit to the chlorine 2p photoelectron spectrum was achieved (Figure 10), with a ratio of bridging chlorides to terminal chlorides Cl_b/Cl_t=1.16. This ratio does not permit an unambiguous choice between the two possible models for this cluster: $(Mo_6Cl_6S_2)Cl_6$ (Cl_b/Cl_t=1.00) and $(Mo_6Cl_7S)SCl_5$ (Cl_b/Cl_t=1.40). Attempts to reproduce the preparation of this compound have failed, leading instead to $(C_5H_5NH)_3[(Mo_6Cl_7S)Cl_6]$. Thus, the substitution reaction in refluxing pyridine is not a practical procedure for cleanly

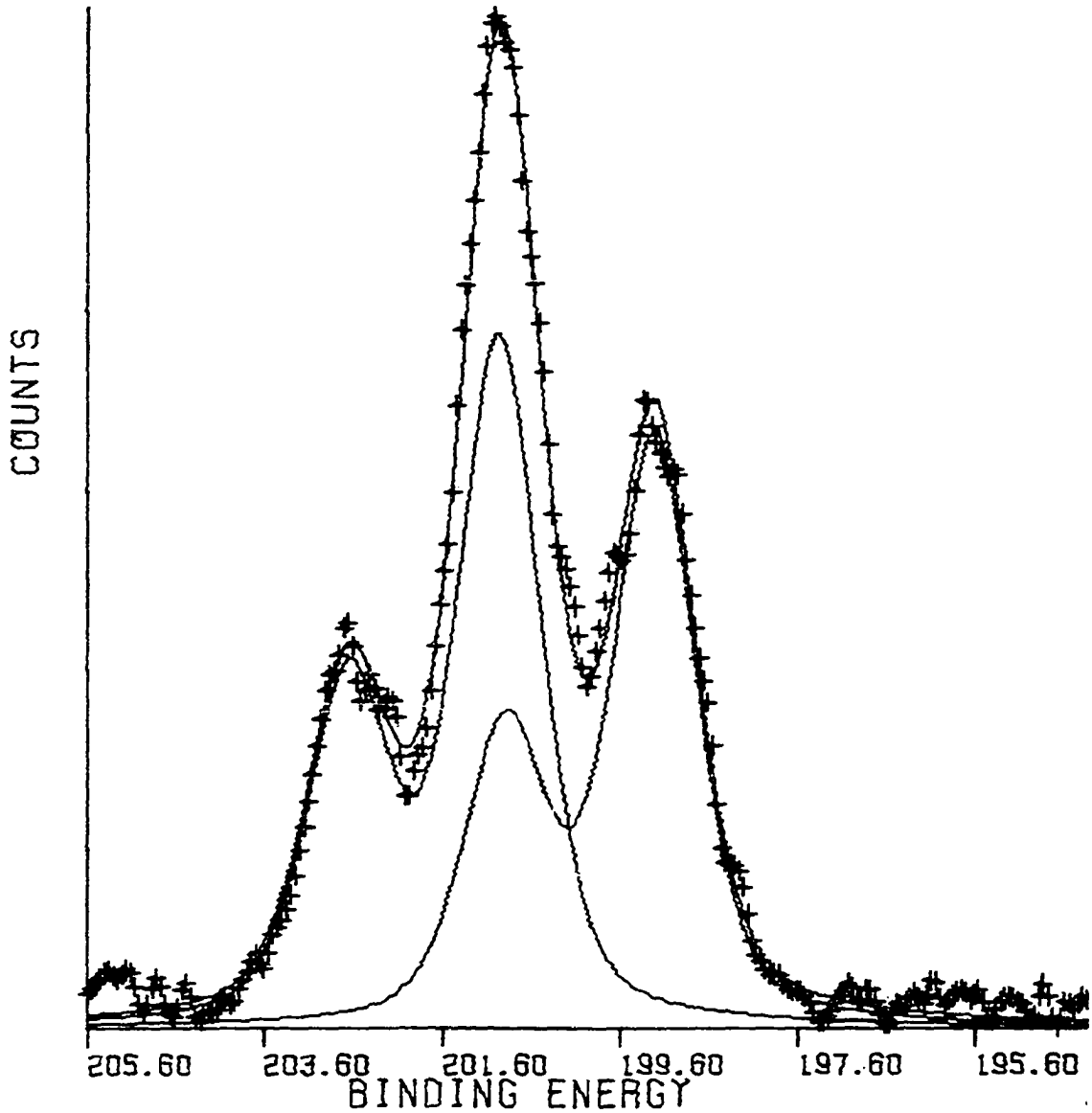

Figure 10. The chlorine 2p photoelectron spectrum of $(H_3O)(C_5H_5NH)_3(Mo_6Cl_{12}S_2)\cdot 5H_2O$

preparing increasingly substituted clusters, viz. $Mo_6Cl_6S_2$, $Mo_6Cl_5S_3$, etc.

In an attempt to determine the maximum extent of the substitution reaction possible under these conditions, Mo_6Cl_{12} was reacted with sixteen equivalents of NaSH in refluxing pyridine. A material having the approximate composition $Mo_6S_5Cl_3(NC_5H_5)_3$ was isolated. Sharp bands characteristic of coordinated pyridine occurred in the infrared spectrum of $(Mo_6S_5Cl_3)(NC_5H_5)_3$. However, the strong infrared absorptions of $Mo_6Cl_8L_6$ clusters (200-400 cm^{-1}) were absent or greatly weakened. The chlorine 2p photoelectron spectrum of $(Mo_6S_5Cl_3)(NC_5H_5)_3$ indicated only one type of chloride in the structure. Attempts to prepare single crystals of this compound suitable for a structure determination were unsuccessful.

An even greater degree of substitution has been achieved by increasing the reaction temperature to 200°C. Since this temperature is 85°C above the boiling point of the pyridine solvent, these reactions were carried out in sealed 13 mm pyrex tubing. Reaction of Mo_6Cl_{12} with eight equivalents of NaSH produced crystals of $(Mo_6S_{\sim 6}Cl_{\sim 2})(NC_5H_5)_6$. The structure of this compound, determined by single crystal x-ray techniques, consists of a Mo_6X_8 cluster with six terminal pyridine ligands. $(Mo_6S_{\sim 6}Cl_{\sim 2})(NC_5H_5)_6$ is the first example of a

$Mo_6X_8L_6$ cluster with fewer than 24 electrons involved in metal-metal bonding.

The powder patterns of $(Mo_6S_5Cl_3)(NC_5H_5)_3$, $(Mo_6S_{\sim 6}Cl_{\sim 2})(NC_5H_5)_6$ and of $(Mo_6S_7Cl)(NC_5H_5)_5$ (prepared in a reaction of Mo_6Cl_{12} with ten equivalents of NaSH and one equivalent of S) are nearly identical. This evidence suggests that these three "compounds" all occur within the range of compositions of a molecular solid solution.

REFERENCES AND NOTES

1. Chevrel, R.; Sergent, M.; Prigent, J. J. Solid State Chem. 1971, 3, 515.

2. Sergent, M.; Chevrel, R. C. R. Hebd. Seances Acad. Sci., Ser. C 1972, 274, 1965.

3. Sergent, M.; Chevrel, R. J. Solid State Chem. 1973, 6, 433.

4. Chevrel, R.; Sergent, M.; Fischer, O. Mater. Res. Bull. 1975, 10, 1169.

5. Schöllhorn, R.; Kümpers, M.; Besenhard, J. O. Mater. Res. Bull. 1977, 12, 781.

6. Flükiger, R.; Baillif, R.; Walker, E. Mater. Res. Bull. 1978, 13, 743.

7. Bars, O.; Guillevic, J.; Grandjean, D. J. Solid State Chem. 1973, 6, 48.

8. Guillevic, J.; Bars, O.; Grandjean, D. J. Solid State Chem. 1973, 7, 158.

9. Marezio, M.; Dernier, P. D.; Remeika, J. P., Corenzwit, E.; Matthias, B. T. Mater. Res. Bull. 1973, 8, 657.

10. Chevrel, R.; Sergent, M.; Prigent, J. Mater. Res. Bull. 1974, 9, 1487.

11. Guillevic, J.; Bars, O.; Grandjean, D. Acta Crystallogr., Sect B 1976, 32, 1338.

12. Fischer, O.; Odermatt, R.; Bongi, G.; Jones, H.; Chevrel, R.; Sergent, M. Phys. Lett. A 1973, 45, 87.

13. Fischer, O.; Jones, H.; Bongi, G., Sergent, M.; Chevrel, R. J. Phys. C. 1974, 7, L450.

14. Foner, S.; McNiff, E. J., Jr.; Alexander, E. J. Phys. Lett. A 1974, 49, 269.

15. Johnston, D. C.; Shelton, R. N. J. Low Temp. Phys. 1977, 26, 561.

16. Lawson, A. C.; Shelton, R. N. Mater. Res. Bull. 1977, 12, 375.

17. Bolz, J.; Crecelius, G.; Maletta, H.; Pobell, F. J. Low Temp. Phys. 1977, 28, 61.

18. Matthias, B. T.; Marezio, M.; Corenzwit, E.; Cooper, A. S.; Barz, H. Science 1972, 175, 1465.

19. Schäfer, H.; von Schnering, H. G.; Tillack, J.; Kuhnen, F.; Wöhrle, H., Baumann, H. Z. Anorg. Allg. Chem. 1967, 353, 281.

20. Von Schnering, H. G. Max Planck Institut für Festkörperfurschung; private communication, 1979.

21. Pauling, L. "The Nature of the Chemical Bond", 3rd ed.; Cornell University Press: Ithaca, New York, 1960, p 256.

22. Pauling, L. "The Nature of the Chemical Bond", p 260.

23. Guggenberger, L. J.; Sleight, A. W. Inorg. Chem. 1969, 8, 2041.

24. Pauling, L. "The Nature of the Chemical Bond", p 246.

25. Pauling, L. "The Nature of the Chemical Bond", p 224.

26. Estimated terminal bond radius of molybdenum = 1.40Å.

27. $PbMo_6S_8$ is an idealized formulation. As determined during the structure refinement, the actual stoichiometry is $Pb_{0.92}Mo_6S_{7.5}$. The sulfur deficiency is limited to the two S in special ($\bar{3}$) positions.

28. Yvon, K. In "Current Topics in Materials Science", 1st ed.; Kaldis, E., Ed.; North-Holland: New York, 1978; Vol. 3, Chapter 2.

29. Cotton, F. A.; Haas, T. E. Inorg. Chem. 1964, 3, 10.

30. Hamer, A. D.; Smith, T. J.; Walton, R. A. Inorg. Chem. 1976, 15, 1014.

31. Andersen, O. K.; Klose, W.; Nohl, H. Phys. Rev. B 1978, 17, 1209.

32. Perrin, A.; Sergent, M.; Fischer, O. Mater. Res. Bull. 1978, 13, 259.

33. Chevrel, R. Ph.D. Dissertation, University of Rennes, 1974.

34. Sergent, M.; Fischer, O.; Decroux, M.; Perrin, C.; Chevrel, R. J. Solid State Chem. 1977, 22, 87.

35. Hauck, J. Mater. Res. Bull. 1977, 12, 1015.

36. Dorman, W. C. Ph.D. Dissertation, Iowa State University, 1974.

37. Sheldon, J. C. Nature 1959, 184, 1210.

38. Cotton, F. A.; Curtis, N. F. Inorg. Chem. 1965, 4, 241.

39. Sheldon, J. C. J. Chem. Soc. 1960, 1007.

40. Schäfer, H.; Plautz, H. Z. Anorg. Allg. Chem. 1972, 389, 57.

41. Lessmeister, P.; Schäfer, H. Z. Anorg. Allg. Chem. 1975, 417, 171.

42. Weissenhorn, R. G. Z. Anorg. Allg. Chem. 1976, 426, 159.

43. Baumann, H.; Plautz, H.; Schäfer, H. J. Less-Common Met. 1971, 24, 301.

44. Sheldon, J. C. J. Chem. Soc. 1962, 410.

45. Lesaar, H.; Schäfer, H. Z. Anorg. Allg. Chem. 1971, 385, 65.

46. Sheldon, J. C. Chem. Ind. (London) 1961, 323.

47. Nannelli, P.; Block, B. P. Inorg. Chem. 1968, 7, 2423.

48. Dorman, W. C.; McCarley, R. E. Inorg. Chem. 1974, 13, 491.

49. Brauer, G. "Handbuch der Präparativen Anorganischen Chemie", 2nd ed.; Ferdinand Enke: Stuttgart, 1960; p 325.

50. Luly, M. H. (1979). "APES, A Fortran Program to Analyze Photoelectron Spectra", US DOE Report IS-4694.

51. Shirley, D. A. Phys. Rev. B 1972, 5, 4709.

52. Rohrbaugh, W. J.; Jacobson, R. A. Inorg. Chem. 1974, 13, 2535.

53. Jacobson, R. A. J. Appl. Crystallogr. 1976, 9, 115.

54. Hubbard, C. R.; Babich, M. W.; Jacobson, R. A. (1977). "A PL/1 Program System for Generalized Patterson Superpositions", US AEC Report IS-4106.

55. Hubbard, C. R.; Quicksall, C. O.; Jacobson, R. A. (1971). "The Fast Fourier Algorithm and the Programs ALFF, ALFFDP, ALFFPROJ, ALFFT, and Friedel", US AEC Report IS-2625.

56. Lapp, R. L.; Jacobson, R. A. (1979). "ALLS, A Generalized Crystallographic Least Squares Program", US DOE Report IS-4708.

57. Hanson, H. P.; Herman, F.; Lea, J. D.; Skillman, S. Acta Crystallogr. 1964, 17, 1040.

58. Templeton, D. H. In "International Tables for X-ray Crystallography", 1st ed.; Macgillavry, C. H. and Rieck, G. D., Ed.; Kynoch Press: Birmingham, England, 1962; Vol. III, Page 215.

59. Michel, J. B. Ph.D. Dissertation, Iowa State University, 1979; Part II.

60. Gill, N. S.; Nuttall, R. H.; Scaife, D. E.; Sharp, D. W. A. J. Inorg. Nucl. Chem. 1961, 18, 79.

61. Mackay, R. A. Ph.D. Dissertation, State University of New York at Stony Brook, 1966.

62. Hogue, R. D.; McCarley, R. E. Inorg. Chem. 1970, 9, 1354.

63. Müller, A.; Sarkar, S.; Bhattacharyya, R. G.; Pohl, S.; Dartmann, M. Angew. Chem. 1978, 90, 564.

64. Walton, R. A. Coord. Chem. Rev. 1976, 21, 63.

65. Walton, R. A. J. Less-Common Metals 1977, 54, 71.

66. Hamer, A. D.; Walton, R. A. Inorg. Chem. 1974, 13, 1446.

67. Best, S. A.; Walton, R. A. Inorg. Chem. 1979, 18, 484.

68. Ebner, J. R.; McFadden, D. L.; Tyler, D. R.; Walton, R. A. Inorg. Chem. 1976, 15, 3014.

69. Johnson, C. K. (1965). "ORTEP, A Fortran Thermal-Ellipsoid Plot Program for Crystal Structure Illustrations", US AEC Report ORNL-3794.

70. Pimentel, G. C.; McClellan, A. L. "The Hydrogen Bond", 1st ed.; W. H. Freeman and Co.: San Francisco, 1960; Chapter 9.

71. Busing, W. R.; Martin, K. O.; Levy, H. A. (1964). "ORFFE, A Fortran Crystallographic Function and Error Program", US AEC Report ORNL-TM-306.

72. Von Schnering, H. G. Z. Anorg. Allg. Chem. 1971, 385, 75.

73. Perrin, C.; Sergent, M.; Le Traon, F.; Le Troon, A. J. Solid State Chem. 1978, 25, 197.

74. Healy, P. C.; Kepert, D. L.; Taylor, D.; White, A. H. J. Chem. Soc., Dalton Trans. 1973, 646.

75. Karcher, B. A.; Jacobson, R. A. Ames Laboratory, Iowa State University; private communication, 1979.

76. Perrin, C.; Sergent, M.; Prigent, J. C. R. Hebd. Seances Acad. Sci., Ser. C 1973, 277, 465.

77. Michel, J. B. Ph.D. Dissertation, Iowa State University, 1979; Part I.

78. Schäfer, H.; Siepmann, R. Z. Anorg. Allg. Chem. 1968, 357, 273.

79. Siepmann, R.; Von Schnering, H. G. Z. Anorg. Allg. Chem. 1968, 357, 289.

80. Simon, A.; Von Schnering, H. G.; Schäfer, H. Z. Anorg. Allg. Chem. 1967, 355, 295.

81. Bateman, L. R.; Blount, J. F.; Dahl, L. F. J. Am. Chem. Soc. 1966, 88, 1082.

82. Imoto, H.; Corbett, J. D. Ames Laboratory, Iowa State University; private communication, 1979.

83. Brenčič, J. V. Z. Anorg. Allg. Chem. 1974, 403, 218.

84. Jackson, R. B.; Streib, W. E. Inorg. Chem. 1971, 10, 1760.

85. Cotton, F. A.; Norman, J. G., Jr. J. Am. Chem. Soc. 1972, 94, 5697.

ACKNOWLEDGEMENTS

A large debt of gratitude is owed to my major professor, Dr. Robert McCarley. He instilled in me a measure of his own enthusiasm for chemistry, thus making my foray into chemical research personally rewarding.

I appreciate the friendship which has been extended to me by the members of my research group. I am grateful to Matt Luly for assistance with the analysis of the photoelectron spectra, to Jim Benson for assistance with x-ray data collection, and to Deb Beckman, Barb Helland, and Doug Powell, who answered many of the questions of a neophyte crystallographer.

Finally, I also appreciate the love and support which have been tendered by my family.